Orientational Effect on the Photophysical Properties of Quaterthiophene – C_{60} Dyads

Paul A. van Hal,[a] Edwin H. A. Beckers,[a] Stefan C. J. Meskers,[a] René A. J. Janssen,*[a] Bruno Jousselme,[b] Philippe Blanchard,[b] and Jean Roncali*[b]

Abstract: Two quaterthiophene–[60]fullerene dyads in which C_{60} is singly (**4TsC**) or doubly (**4TdC**) connected to the inner β-position of the terminal thiophene rings have been synthesized. The electronic properties of these donor–acceptor compounds were analyzed by UV/Vis spectroscopy and cyclic voltammetry, and their photophysical properties in solution and in the solid state by (time-resolved) photoluminescence (PL) and photoinduced absorption (PIA) spectroscopy. Both the flexible and geometrically constrained **4TsC** and **4TdC** dyads exhibit photoinduced charge transfer from the quaterthiophene to the fullerene in toluene and *o*-dichlorobenzene (ODCB). In toluene, charge transfer occurs in both dyads by an indirect mechanism, the first step of which is a singlet-energy transfer from the $4T(S_1)$ state to the $C_{60}(S_1)$ state. In the more polar ODCB, direct electron transfer from $4T(S_1)$ competes with energy transfer, and both direct and indirect charge transfers are observed. The geometrical fixation of the donor and acceptor chromophores in **4TdC** results in rate constants for energy and electron transfer that are more than an order of magnitude larger than those of the flexible **4TsC** system. For both dyads, charge recombination is extremely fast, as inferred from picosecond-resolved temporal evolution of the excited state absorption of the $4T^{\bullet+}$ radical cation both in toluene and ODCB.

Keywords: donor–acceptor systems · electron transfer · fullerenes · laser spectroscopy · oligothiophenes

Introduction

Composite films of π-conjugated polymers (electron donor) and fullerenes (electron acceptor) have been used successfully as the active layer in organic solar cells.[1] Photoinduced subpicosecond forward electron transfer between the donor and acceptor in these blends[2] leads to an initial quantum efficiency for charge separation close to unity. Importantly, the resulting charges have lifetimes up to the millisecond time range[3] that allow transport and collection of the charges at the electrodes.

In addition to charge transfer, other phenomena such as thermal decay of the excited state and energy transfer, can follow photoexcitation of donor–acceptor molecules and thereby influence the efficiency of charge generation. In oligo(thienylenevinylene)–C_{60} dyads,[4] charge formation competes with fast thermal deactivation of the excited oligomer. For oligo(*p*-phenylenevinylene)–C_{60}[5] and oligothiophene–C_{60},[6] ultrafast energy transfer ($k_{ET} \approx 10^{13}\ s^{-1}$) from the singlet excited state of the π-conjugated oligomer to the singlet excited state of the fullerene moiety precedes an indirect charge transfer reaction in a polar environment. In solution, the rate constant for this indirect charge transfer is more than two orders of magnitude lower than that of the electron transfer observed in a solid-state composite film of a π-conjugated polymer and a fullerene derivative.[2] In these composite films, the charge transfer is likely to occur directly from the singlet excited state of the polymer, because no indication for a possible competitive energy transfer is observed.

The much higher electron transfer rates observed in the solid state can be related to the relative spatial arrangement of the donor and acceptor chromophores, because in the solid state a face-to-face orientation of the chromophores is possible.

In recent years, extensive studies on covalently linked, conjugated oligomer–C_{60} dyad molecules have been performed in order to better understand the photophysics of these processes.[4–8] The molecular design of these conjugated oligomer–C_{60} dyads allows precise control of the interactions between donor and acceptor moieties and thus the restriction of the photophysical processes to exactly one donor–acceptor

[a] Prof. R. A. J. Janssen, P. A. van Hal, E. H. A. Beckers, Dr. S. C. J. Meskers
Laboratory of Macromolecular and Organic Chemistry
Eindhoven University of Technology
PO Box 513, 5600 MB Eindhoven (The Netherlands)
Fax: (+31) 40-2451036
E-mail: r.a.j.janssen@tue.nl

[b] Prof. J. Roncali, B. Jousselme, Dr. P. Blanchard
Ingénierie Moléculaire et Matériaux Organiques
CNRS UMR 6501, Université d'Angers
2 Boulevard Lavoisier, 49045 Angers Cedex (France)
E-mail: jean.roncali@univ-angers.fr

  0947-6539/02/0823-5415 $ 20.00+.50/0

couple in dilute solution. Results obtained on porphyrin–C_{60}[9] and aniline–C_{60}[10] dyads underlined the importance of the geometry of the linker group. The distance between the donor and acceptor moieties and their mutual orientation are also crucial parameters for the rate of charge generation, transfer, and recombination. For example, whereas porphyrin–C_{60} dyads connected by a single bridge show charge-transfer rate constants in the range of $10^{10}\,s^{-1}$, this value increases by one order of magnitude for a doubly bridged face-to-face dyad.[11]

We report here the synthesis and photophysical properties of two donor–acceptor dyads in which a quaterthiophene (**4T**) was singly (**4TsC**) or doubly (**4TdC**) attached to a C_{60} group by a single or a double Bingel reaction. These different modes of attachment result in a different relative spatial orientation of the 4T and C_{60} chromophores, with a completely free orientation in the former case and a geometrical constraint imposing a face-to-face orientation in the latter case.

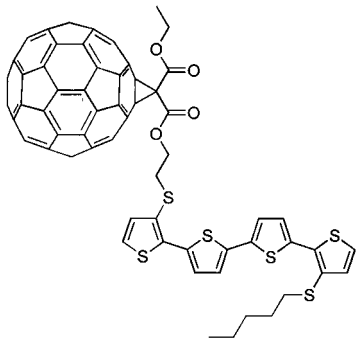

4TsC

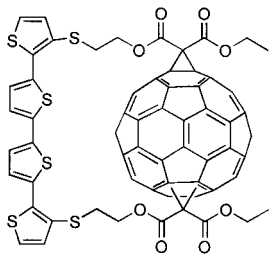

4TdC

The photophysical properties of these two dyads have been analyzed by using their individual constituent chromophores, namely, dipentylsulfanyl-4T (**4TP**) (Schemes 1 and 2) and the C_{60} adducts **C_{60}s** and **C_{60}d** as reference compounds. (Time-resolved) photoluminescence (PL) and (time-resolved) photoinduced absorption (PIA) spectroscopy in solvents with different permittivity revealed significant differences in the rates for both energy and electron transfer. The energetics of the direct and indirect electron-transfer reactions in solution can be rationalized on the basis of the Marcus theory.

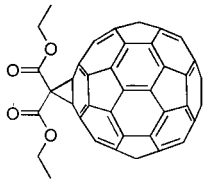

C_{60}s

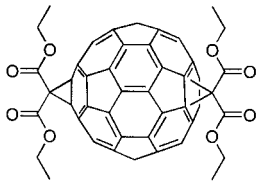

C_{60}d

Results and Discussion

Synthesis: The synthesis of the target dyads and reference compounds is depicted in Schemes 1 and 2. 3-(2-Cyanoethylsulfanyl)thiophene (**5**) was prepared in 83% yield from 3-bromothiophene (**6**) in a one-pot reaction involving lithium/bromine exchange with *n*-butyllithium at low temperature and insertion of elemental sulfur to generate the 3-thiophenethiolate, which was alkylated with 3-bromopropionitrile (Scheme 1).[12] Selective bromination of **5** with *N*-bromosuccinimide (NBS) in dimethylformamide (DMF) gave the 2-bromothiophene (**4**) in 85% yield. Treatment of bithiophene (**3**) with *n*-butyllitium and tributylstannylchloride afforded bis(tributylstannyl)bithiophene (**2**),[13] which was then coupled to **4** in a Stille reaction in the presence of a palladium catalyst to give the key compound bis(cyanoethylsulfanyl)quaterthiophene (**1**) in 73% yield (Scheme 1).

Deprotection of one thiolate group of **1** with one equivalent of CsOH followed by reaction with iodopentane gave **7** in 52% yield together with 16% of the dipentylsulfanyl compound **4TP** (Scheme 2). Compound **9** was then obtained by deprotection of the remaining thiolate group of **7** and treatment with 2-bromoethanol. Application of the same reaction sequence to **1** with two equivalents of CsOH leads to quaterthiophene **8** bearing two terminal hydroxyl groups.

Esterification of **8** and **9** with 3-chloro-3-oxoethylpropanoate gave mono- and diesters **10** and **11**, which were subsequently subjected to a Bingel reaction[14] in the presence of iodine and 1,8-diazabicyclo[5.4.0]undec-7-ene (DBU) to give the target dyads **4TsC** and **4TdC** in 42 and 35% yield, respectively (Scheme 2). Because of the lack of regioselectivity of the second Bingel reaction, **4TdC** was obtained as a mixture of several isomers.

The reference compounds **C_{60}s** and **C_{60}d** were synthesized by the method described by Hirsch et al.[15] Again the product

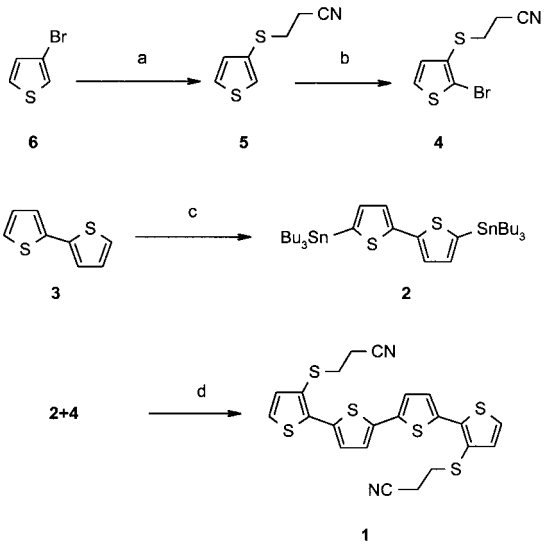

Scheme 1. Synthesis of precursor **1**. a) 1. *n*BuLi/Et_2O, −78 °C; 2. S_8; 3. $NC(CH_2)_2Br$, 0 °C, N_2. b) NBS/DMF, RT, N_2. c) 1. *n*BuLi/THF, −78 °C; 2. Bu_3SnCl, RT, N_2. d) $[Pd(PPh_3)_4]$/toluene, reflux, N_2.

0947-6539/02/0823-5416 $ 20.00+.50/0 *Chem. Eur. J.* **2002**, *8*, No. 23

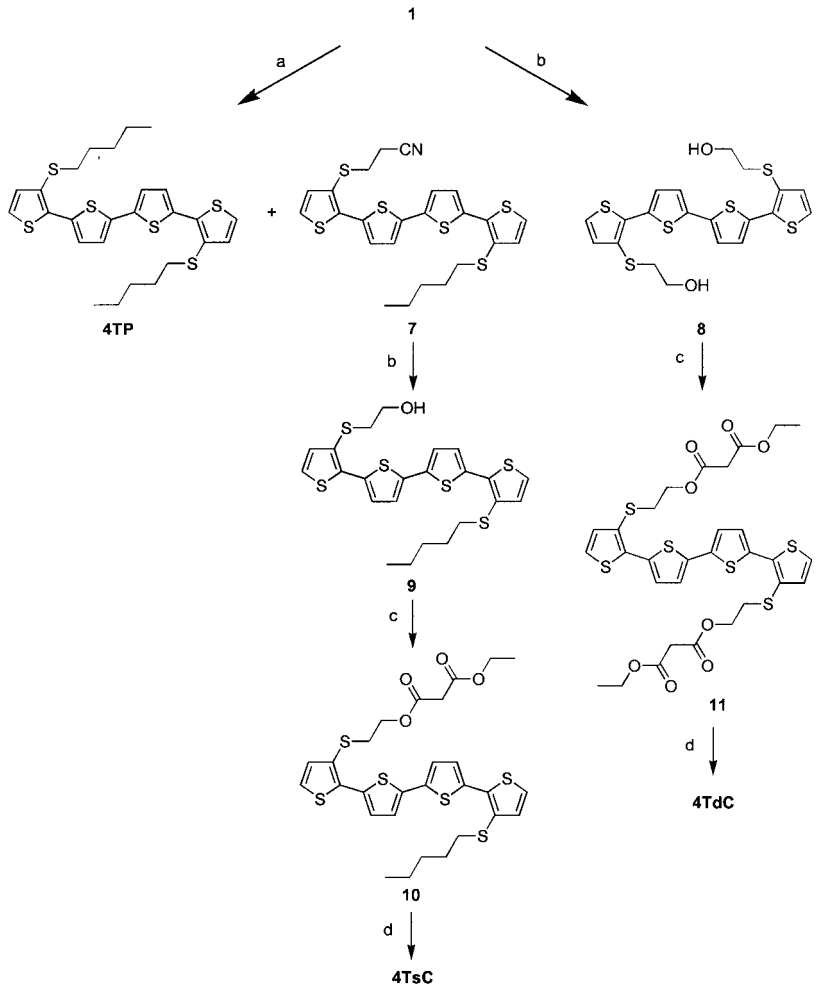

Scheme 2. Synthesis of **4TP**, **4TsC**, and **4TdC**. a) 1. CsOH/MeOH, DMF, 2. $nC_5H_{11}I$, RT, N_2. b) 1. CsOH/MeOH, DMF; 2. $Br(CH_2)_2OH$, RT, N_2. c) Ethyl 3-chloro-3-oxopropionate, pyridine/CH_2Cl_2, reflux, N_2. d) DBU, I_2, C_{60}/toluene, N_2.

of the double Bingel reaction was obtained as a mixture of isomers.

Energy levels of singlet and triplet states of quaterthiophene and fullerene compounds: The UV/Vis spectrum of **4TP** shows a maximum at $\lambda = 405$ nm and an onset at $\lambda = 475$ nm (Figure 1). Fullerene **C_{60}s** has a strong absorption at 330 nm, a peak at 427 nm, and a weak absorption at 690 nm. The UV/Vis spectrum of **C_{60}d** shows less fine structure and exhibits a broad absorption in the 300–330 nm region, a band at 422 nm, and a weak band around 693 nm. The optical absorption spectra of **4TsC** and **4TdC** are very similar to the superposition of the spectra of the **4TP** and C_{60} reference compounds, and this suggests that the electronic coupling between the donor and acceptor chromophores in the ground state is very weak (Figure 1). The UV/Vis spectra of **4TsC** and **4TdC** show that selective excitation of the fullerene is possible above 500 nm. The 4T chromophore of the dyads can be preferentially, but not completely selectively, excited in the 400–420 nm region.

In toluene, **4TP** emits yellow-green light with a peak at 473 nm, a maximum at 504 nm, and a shoulder at 542 nm (Figure 2a). Both **C_{60}s** and **C_{60}d** have low quantum yields for photoluminescence and show weak emissions at 698 and 704 nm, respectively, typical of fullerene derivatives (Figure 2c).[16] Both the quantum yield and the emission wavelength do not change significantly when toluene is replaced by ODCB (Figure 2b and d). Based on the emission spectra, the energy levels of the **4TP**(S_1), **C_{60}s**(S_1), and **C_{60}d**(S_1) singlet states are set to 2.63, 1.78, and 1.75 eV, respectively.

The energy levels of the fullerene triplet states were determined from their phosphorescence spectra. Compounds **C_{60}s** and **C_{60}d** were dissolved in a 2:1:1 mixture of methylcyclohexane, 2-methyltetrahydrofuran, and iodoethane and cooled to 80 K.[17, 18] For both C_{60} reference compounds, the fluorescence is reduced dramatically in this matrix, while a new phosphorescent emission band appears at 825 nm (Figure 3),[16b, 18] which corresponds to a $C_{60}(T_1)$ state energy of 1.50 eV for both **C_{60}s** and **C_{60}d**. The triplet state of **4TP** was assumed to be comparable to that of a related α-quaterthiophene and lies significantly higher than that of the fullerene (1.81 eV).[19]

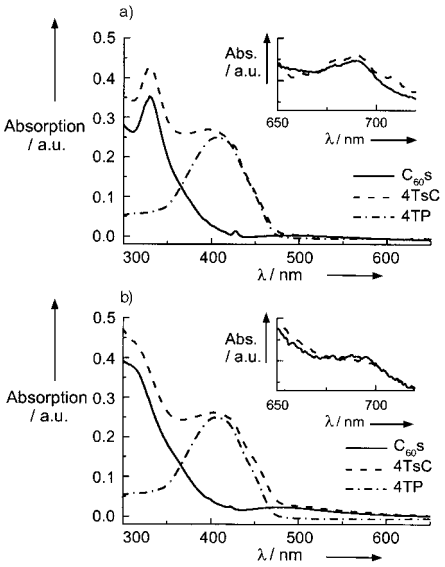

Figure 1. UV/Vis absorption spectra of **4TsC** (a) and **4TdC** (b) and their reference compounds **4TP**, **C_{60}s**, and **C_{60}d** in toluene at room temperature.

  0947-6539/02/0823-5417 $ 20.00+.50/0

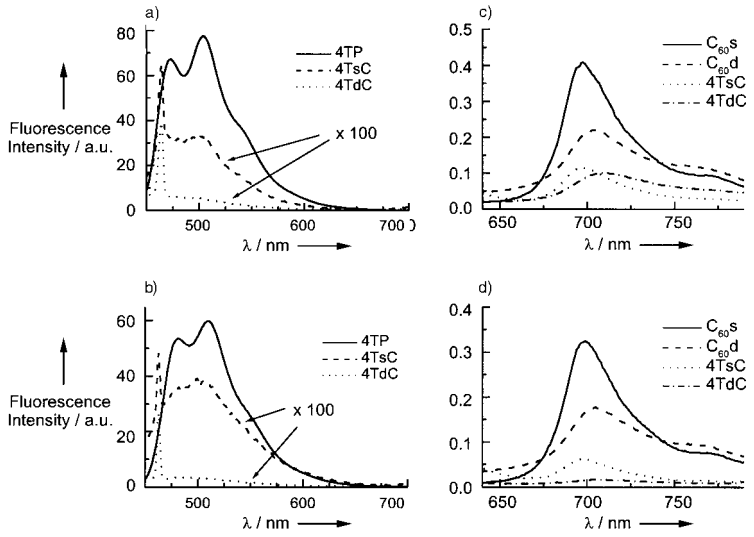

Figure 2. Photoluminescence spectra of 4T emission (a and b) and fullerene emission (c and d) for **4TP**, **4TsC**, **4TdC**, $\mathbf{C_{60}s}$, and $\mathbf{C_{60}d}$ upon excitation at $\lambda = 407$ nm in toluene (a and c) and at $\lambda = 405$ nm in ODCB (b and d) at room temperature. All graphs are corrected for optical density at the excitation wavelength.

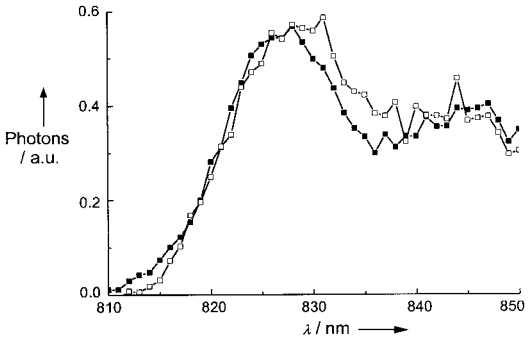

Figure 3. Phosphorescence spectra at $T = 80$ K of $\mathbf{C_{60}s}$ (■) and $\mathbf{C_{60}d}$ (□) in methylcyclohexane:2-methyltetrahydrofuran:iodoethane (2:1:1).

The cyclic voltammograms of **4TsC** and **4TdC** shows two reversible oxidation waves corresponding to the successive generation of the **4T** radical cation and dication. The redox peak potentials (Table 1) are slightly more positive than those of the **4TP** reference compound but quite similar to those of the corresponding ester-containing quaterthiophenes **10** and **11**. This difference presumably reflects the electron-withdrawing effect of the ester groups. For both dyad molecules, reversible reduction waves are observed around -0.60 and -1.00 V (Table 1). No attempts to reach the further reduced states of the C_{60} systems were made. In both cases, comparison with the corresponding reference compounds $\mathbf{C_{60}s}$ and $\mathbf{C_{60}d}$ reveals a slight negative shift of the redox potentials, which might be indicative of some weak through-space interaction between the 4T and the C_{60} moieties in the dyads. It can also be attributed to small differences in solvation, because in the dyads and in **4TP**, **10**, and **11**, the solvent-accessible surface differs.

Table 1. Cathodic (E_{pc2}, E_{pc1}) and anodic (E_{pa1}, E_{pa2}) peak potentials [V vs Ag/AgCl] for the reduction and oxidation of the various quaterthiophenes and C_{60} derivatives. Electrolytic medium 0.10 M Bu_4NPF_6/CH_2Cl_2, scan rate 100 mV s^{-1}.

Compound	E_{pc2}	E_{pc1}	E_{pa1}	E_{pa2}
4TP	–	–	0.89	1.10
10	–	–	0.92	1.12
4TsC	−1.00.	−0.61	0.92	1.13
$\mathbf{C_{60}s}$	−0.97	−0.59	–	–
11	–	–	0.97	1.19
4TdC	−1.07	−0.69	0.97	1.21
$\mathbf{C_{60}d}$	−1.05	−0.68	–	–

Photoluminescence quenching in the dyads: The degree of quenching of photoluminescence of both chromophores, measured upon selective photoexcitation of 4T or C_{60}, within the dyad molecules can be used to determine the extent of energy and charge transfer relative to the intrinsic decay of their excited states and to differentiate between direct and indirect charge-transfer pathways (Scheme 3). The fluorescence spectra of both dyads were recorded in two different solvents [toluene ($\varepsilon = 2.38$) and ODCB ($\varepsilon = 9.93$)], because charge separation is known to depend on polarity.[20]

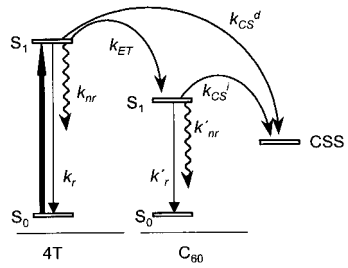

Scheme 3. Photophysical pathways for energy transfer (k_{ET}), direct (k_{CS}^d), and indirect (k_{CS}^i) electron transfer after excitation of the donor. Intrinsic radiative (k_r) and nonradiative (k_{nr}) decay of the individual chromophores are shown.

Photoexcitation of the 4T moiety of both dyads reveals considerable quenching of the 4T fluorescence (Figure 2a and b). In both solvents, the residual 4T emission is about ten times larger for the flexible, singly bridged **4TsC** than for the doubly linked **4TdC** dyad. Quenching of the 4T fluorescence reflects the sum of the rates for energy transfer (k_{ET}) and direct charge transfer (k_{CS}^d) relative to the normal radiative (k_r) and nonradiative (k_{nr}) decay of **4TP** (Scheme 3). Upon excitation of the 4T moieties in **4TsC** and **4TdC** at 405 nm, emission of the fullerene moiety is also observed (Figure 2c and d). Apart from some direct excitation of the fullerene moiety, this emission is mainly caused by sensitization of the $C_{60}(S_1)$ state by singlet-energy transfer from the initial $4T(S_1)$ state. However, the fullerene emission of the dyads is weaker than that of the $\mathbf{C_{60}s}$ and $\mathbf{C_{60}d}$ reference compounds. This quenching can be explained by an electron-transfer reaction, either

0947-6539/02/0823-5418 $ 20.00+.50/0 *Chem. Eur. J.* **2002**, *8*, No. 23

from the initial 4T(S_1) state (k_{CS}^d, Scheme 3) or from the C_{60}(S_1) state (k_{CS}^i, Scheme 3) formed by energy transfer (k_{ET}, Scheme 3). In toluene, the fullerene emission of both dyads is quenched by a factor of 2–4 (Figure 2c). Replacing toluene by the more polar ODCB only marginally affects the intensity of the residual 4T photoluminescence, but produces a further decrease in the C_{60} luminescence (Figure 2d). The quenching of fullerene emission in ODCB is significantly larger for **4TdC** than for **4TsC**.

To specify the charge transfer in terms of direct or indirect pathways, the donor and acceptor parts of the dyads were selectively excited. Direct electron transfer from 4T(S_1) and indirect electron transfer from C_{60}(S_1) can be quantified by comparing the acceptor luminescence after selective excitation of the donor (at 405 nm) or the acceptor (at 520 nm) (Table 2). In toluene, the residual C_{60} luminescence of both

Table 2. Rate constants for energy transfer (k_{ET}), indirect charge transfer (k_{CS}^i), and direct charge transfer (k_{CS}^d) calculated from the PL quenching of donor (Q_D) or acceptor (Q_A). The excited moiety of the DA dyad is indicated by an asterisk.

Sample	Solvent	Q_D(D*A)	Q_A(DA*)	Q_A(D*A)	k_{ET} [ns^{-1}]	k_{CS}^i [ns^{-1}]	k_{CS}^d [ns^{-1}]	k_{CS}^{i}[a] [ns^{-1}]
4TsC	toluene	250	3.6	3.6	520	1.7	< 1	1.0
4TdC	toluene	> 1600	2.3	2.3	> 3300	0.8	< 1	1.1
4TsC	ODCB	160	4.0	5.3	240	2.1	76	2.1
4TdC	ODCB	> 2000	8.3	11.1	> 3000	3.8	> 1010	2.8

[a] Photoluminescence lifetime obtained from Equations (4) and (5).

4TsC and **4TdC** is independent of the photoexcited moiety of the dyad. This implies that the indirect electron-transfer process dominates and is preceded by fast singlet-energy transfer to the C_{60}(S_1) state. However, in ODCB the fullerene emission of both dyads is reduced to a larger extent when the 4T donor is excited as compared to selective excitation of the fullerene acceptor. This difference results from direct relaxation of 4T(S_1) to the charge-separated state (CSS) (k_{CS}^d, Scheme 3).

The excitation spectra of the fullerene emission (Figure 4) show whether electron transfer occurs directly from the

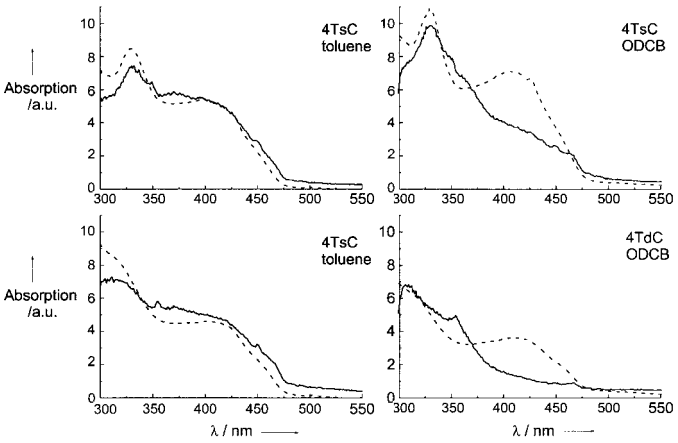

Figure 4. Photoluminescence excitation spectra (——) for **4TsC** (top; $\lambda_{em} = 698$ nm) and **4TdC** (bottom; $\lambda_{em} = 705$ nm) in toluene (left) and ODCB (right) at room temperature compared with UV/Vis absorption spectra (- - - -).

4T(S_1) state or indirectly via the C_{60}(S_1) state following a singlet-energy transfer process. In toluene, the excitation spectra of the C_{60} fluorescence dyads are similar to their UV/Vis absorption spectra (Figure 4, left). This indicates that the residual C_{60} emission can originate from excitation of the 4T or the C_{60} chromophore, and that a full energy-transfer reaction from 4T(S_1) to C_{60}(S_1) occurs prior to a charge-transfer reaction. However, in ODCB, the absorption and excitation spectra are no longer similar. Notably, the characteristic absorption peak of the 4T molecule with a maximum at $\lambda = 405$ nm is drastically reduced in the excitation spectra for both dyads (Figure 4, right). Hence, in ODCB, excitation of the 4T moiety of both dyads does not result in a full population of the C_{60}(S_1) state, because direct charge transfer from the 4T moiety to the charge-separated state competes with singlet-energy transfer to C_{60}(S_1).

The steady-state photoluminescence shows that in toluene singlet-energy transfer dominates the decay of the 4T(S_1) state in **4TsC** and **4TdC**, while in ODCB energy and electron transfer are competitive processes.

Rate constants for energy and electron transfer: Time-correlated single-photon counting (TCSPC) was used to determine the singlet-state lifetimes of **4TP**, **C_{60}s**, and **C_{60}d** by recording the temporal decay of the fluorescence after excitation at 400 nm. Photoexcitation at 400 nm in both toluene and ODCB results in singlet excited state lifetimes τ of about 0.5 ns for **4TP** and 1.5–2.0 ns for the C_{60} derivatives.[21]

Transfer rates from fluorescence quenching: The rate constants for the various transfer processes can be determined by combining the lifetimes of the singlet excited states of the isolated chromophores and the degree of photoluminescence quenching of the dyads. Assuming selective photoexcitation of the chromophores, the contributions of energy transfer and of direct and indirect electron transfer can be calculated by Equations (1)–(3).

$$k_{ET} = \frac{Q_A(DA*)Q_D(D*A)}{Q_A(D*A)\tau_D} \quad (1)$$

$$k_{CS}^i = \frac{Q_A(DA*) - 1}{\tau_A} \quad (2)$$

$$k_{CS}^d = \frac{Q_D(D*A) - 1}{\tau_D} - k_{ET} \quad (3)$$

Here τ_D and τ_A are the singlet-state lifetimes of the isolated donor and acceptor molecules, respectively, and Q_D(D*A), Q_A(D*A), and Q_A(DA*) represent the quenching ratios for the donor (Q_D) or acceptor (Q_A) photoluminescence after selective excitation of the donor (D*A) or the acceptor (DA*).[22] For the quenching ratios listed in Table 2, these equations reveal that upon excitation of the 4T moiety of both dyads an indirect electron transfer occurs in toluene with a rate on the order of $k_{CS}^i = 10^9$ s^{-1} following fast singlet-energy transfer from 4T(S_1) to C_{60}(S_1) with a rate of $k_{ET} > 10^{11}$ s^{-1}. For **4TdC** the energy-transfer rate constant is even one order of magnitude higher than for **4TsC**. In ODCB, the rates for energy transfer for both dyads are comparable to those

measured in toluene. For indirect electron transfer in ODCB the rate is similar to that found in toluene for **4TsC**, but is four times larger for **4TdC**. For direct charge transfer (k_{CS}^{d}) the rate for **4TdC** ($k_{CS}^{d} > 10^{12}\ s^{-1}$) is more than one order of magnitude larger than for **4TsC**.

Transfer rates from fluorescence lifetimes: The rates for indirect charge transfer (k_{CS}^{i}), as determined from the fluorescence quenching Q_A(DA*) and the acceptor lifetime τ_A by using Equation (2), can be compared to rates obtained from time-resolved fluorescence. In this experiment, the lifetime of the fullerene emission of the dyad ($\tau_{A,dyad}$) is recorded and compared to that of the acceptor (τ_A) to give an estimate for the rate constant [Eq. (4)].

$$k_{CS}^{i} = \frac{1}{\tau_{A,dyad}} - \frac{1}{\tau_A} \quad (4)$$

The lifetimes of the residual fullerene emission around 700 nm for **4TsC** and **4TdC** amount to 610 and 580 ps in toluene, and 350 and 300 ps in ODCB (Table 2). The values of k_{CS}^{i} obtained from the lifetimes [Eq. (4)] are similar to those obtained from quenching [Eq. (2)] for both solvents (Table 2).

In principle, the lifetime of the residual 4T emission ($\tau_{D,dyad}$) of the two dyads can be used in an analogous fashion to determine the sum of k_{ET} and k_{CS}^{d} [Eq. (5)].

$$k_{ET} + k_{CS}^{d} = \frac{1}{\tau_{D,dyad}} - \frac{1}{\tau_D} \quad (5)$$

However, the determination of $\tau_{D,dyad}$ appeared to be limited by the time resolution of the TCSPC technique (ca. 10 ps). This results in a lower limit of $k_{ET} + k_{CS}^{d} \geq 10^{11}\ s^{-1}$, consistent with the results obtained from Equations (1) and (3) for both solvents.

In conclusion, photoluminescence quenching and lifetime studies have shown that both energy-transfer and direct charge-transfer rates are about ten times larger for **4TdC** than for **4TsC**.

Near-steady-state photoinduced absorption (PIA) spectroscopy: Near-steady-state photoinduced absorption spectroscopy, which probes the optical spectra of excited states with lifetimes in the micro- and millisecond time domain, was used to obtain direct spectral evidence of charge separation within the dyads. The two dyads were investigated in the solid state and in solution. Furthermore, mixtures of **4TP** with **C_{60}s** or **C_{60}d** were investigated in toluene, ODCB, and benzonitrile.

PIA in the solid state: The photoinduced absorption spectra, recorded at 80 K with excitation at 458 nm, of drop-cast films of **4TsC** and **4TdC** exhibit excited-state absorptions at 0.98, 1.20, and 1.74 eV (Figure 5). The 1.20 eV peak is characteristic for a $C_{60}^{\bullet -}$ radical anion, while the bands at 0.98 and 1.74 eV are assigned to the low-energy (LE) and high-energy (HE) absorption bands of a $4T^{\bullet +}$ radical cation.[23, 24] The observation of the spectral characteristics of both positive and negative charge carriers gives a strong support to the proposed charge-transfer process. Since a 1.74 eV band can also originate from a C_{60} triplet absorption, the charge separation is more convincingly evidenced by the 0.98 and

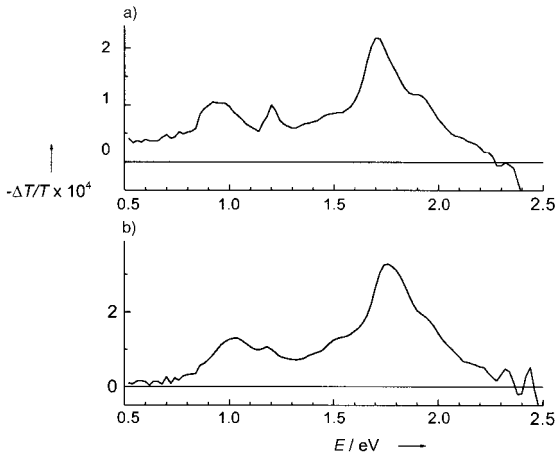

Figure 5. PIA spectra of drop-cast films of **4TsC** (a) and **4TdC** (b). $\lambda_{ex} =$ 458 nm, modulation frequency 275 Hz, excitation intensity 25 mW, $T =$ 80 K.

1.20 eV bands of $4T^{\bullet +}$ and $C_{60}^{\bullet -}$. Increasing the excitation intensity I results in a near square root increase of all PIA bands ($-\Delta T \sim I^{\alpha}$; $\alpha = 0.44$) for both dyads, indicative of bimolecular recombination of a nongeminate pair of opposite charges in the films. The intensity of the PIA bands of both molecules decreases with increasing modulation frequency in the whole range studied (30 – 4000 Hz), consistent with a distribution of lifetimes extending into the millisecond time domain.[3c] The similar intensity and frequency dependence indicates that all bands have a similar origin, and supports the assignment of the 1.74 eV band to the $4T^{\bullet +}$ radical cation. The long lifetime of the charge-separated state in the solid state at low temperatures is interpreted as follows. A small percentage of intramolecular geminate electron – hole pairs will dissociate into a more distant pair of free charges by electron transfer to neighboring dyads. Trapping of these charges in a local minimum will result in a metastable charge-separated state, as recombination of hole and electron is now a thermally activated process.

PIA of reference molecules and their mixtures in solution: First, the reference compounds **4TP**, **C_{60}s**, and **C_{60}d** were studied with PIA in dilute (2×10^{-4} M) solutions [toluene ($\varepsilon =$ 2.38), ODCB ($\varepsilon = 9.93$), and benzonitrile ($\varepsilon = 25.18$)] to investigate their individual photophysical properties and their excited-state behavior in 1:1 (molar ratio) mixtures of donor and acceptor. In the mixtures, selective photoexcitation of the fullerene compound was achieved by exciting at 528 nm.

Photoexcitation of solutions containing **C_{60}s** or **C_{60}d** resulted in a characteristic broad C_{60} triplet absorption band at 1.74 eV ($-\Delta T/T \approx 10^{-4}$), assigned to a $T_n \leftarrow T_1$ excited-state absorption (Figure 6, bottom graph).[25] The fullerene triplet state has a lifetime on the order of 100 μs.[18] The PIA spectrum of **4TP** shows an intense broad band with a maximum at 2.00 eV ($-\Delta T/T \approx 4 \times 10^{-3}$) and a shoulder at 1.70 eV (not shown). These excited-state absorptions are assigned to the $T_n \leftarrow T_1$ transition of the $4T(T_1)$ state.[26] The linear increase of the PIA bands with increasing excitation intensity ($-\Delta T \sim I$), indicates a monomolecular decay mech-

0947-6539/02/0823-5420 $ 20.00+.50/0 *Chem. Eur. J.* **2002**, *8*, No. 23

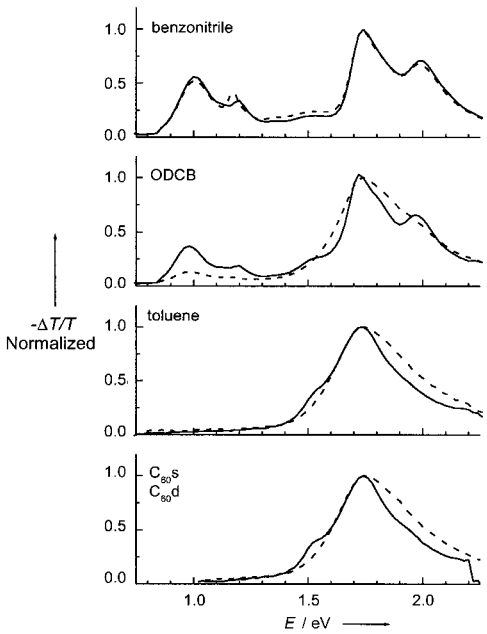

Figure 6. PIA spectra of mixtures of **4TP/C_{60}s** (——) and **4TP/C_{60}d** (----) in toluene, ODCB, and benzonitrile at room temperature. The PIA spectra of the individual C_{60} reference compounds are shown in the bottom graph. $\lambda_{ex} = 528$ nm, modulation frequency 275 Hz, and excitation intensity 25 mW. All spectra have been corrected for detector sensitivity, fluorescence, and normalized on the intensity at 1.74 eV.

anism. The frequency dependence of the PIA bands resulted in a 4T(T_1) lifetime of 160 μs.

Figure 6 shows the PIA spectra of **4TP/C_{60}s** and **4TP/C_{60}d** mixtures in different solvents, normalized to the 1.74 eV band.[25] In toluene, photoexcitation of a 1:1 mixture of **4TP** and **C_{60}s** at 458 nm (mainly 4T absorption) or 528 nm (C_{60} absorption) results in the formation of the $C_{60}(T_1)$ state, as evidenced by the characteristic $T_n \leftarrow T_1$ transition, which exhibits a monomolecular decay mechanism and a lifetime of about 100 μs. This spectrum and, in particular, the absence of signals of 4T(T_1) imply that the $C_{60}(T_1)$ state lies below 4T(T_1) and that triplet-energy transfer occurs in solution from 4T(T_1) to form $C_{60}(T_1)$. This is consistent with the triplet energies of **4TP** (1.81 eV) and **C_{60}s** (1.50 eV), as determined above. In the more polar solvents ODCB and benzonitrile the bands of $4T^{\bullet+}$ at 0.98 and 1.74 eV[23, 24] and of $C_{60}^{\bullet-}$ at 1.20 eV are clearly visible. Moreover, the bands of $4T^{\bullet+}$ are roughly two to three times more intense than the $C_{60}^{\bullet-}$ absorption, in accordance with reported molar absorption coefficients of closely related ions ($4T^{\bullet+}$: 33 500 $M^{-1}cm^{-1}$; $C_{60}^{\bullet-}$: 12 000 $M^{-1}cm^{-1}$).[23, 27] In benzonitrile, a tenfold intensification of the PIA bands ($-\Delta T/T \approx 1.5 \times 10^{-3}$) is observed relative to ODCB ($-\Delta T/T \approx 1.5 \times 10^{-4}$), which reflects the favorable formation of charges in a more polar solvent. In both solvents, all PIA bands show the same dependence on the modulation frequency, that is, the cation and anion radicals originate from and recombine by the same processes. The charge-separated states have lifetimes on the order of 2 ms. The PIA bands increase with increasing excitation intensity according to a near square root dependence ($-\Delta T \sim I^{\alpha}$; $\alpha \approx 0.6-0.7$).

Next, mixtures of **4TP** with **C_{60}d** instead of **C_{60}s** were studied. In toluene, the $C_{60}(T_1)$ state is formed, as shown by the typical excited-state absorptions of C_{60} triplet species (Figure 6) with monomolecular decay and a lifetime of 100 μs. The observation of $C_{60}(T_n \leftarrow T_1)$ is in agreement with the lower energy of the **C_{60}d**(T_1) state compared to the **4TP**(T_1) state. In benzonitrile, strong bands ($-\Delta T/T \approx 1.5 \times 10^{-3}$) of $4T^{\bullet+}$ and **C_{60}d**$^{\bullet-}$ are observed, together with a bimolecular decay mechanism and lifetimes on the order of 2–3 ms. In ODCB, the PIA spectrum of **4TP/C_{60}d** displays mainly the $C_{60}(T_n \leftarrow T_1)$ absorption ($-\Delta T/T \approx 1.5 \times 10^{-4}$) spectrum with an additional small absorption of the $4T^{\bullet+}$ radical cation at 0.98 eV ($-\Delta T/T \approx 1.5 \times 10^{-5}$). This result indicates that, in ODCB, the **4TP**$^{\bullet+}$/**C_{60}d**$^{\bullet-}$ charge-separated state is close in energy to the **C_{60}d**(T_1) state.

PIA of donor–acceptor dyads in solution: The PIA spectra of **4TsC** and **4TdC** in toluene and ODCB are depicted in Figure 7 together with the PIA spectra of **C_{60}s** and **C_{60}d**. All spectra were measured by exciting at 458 nm and corrected

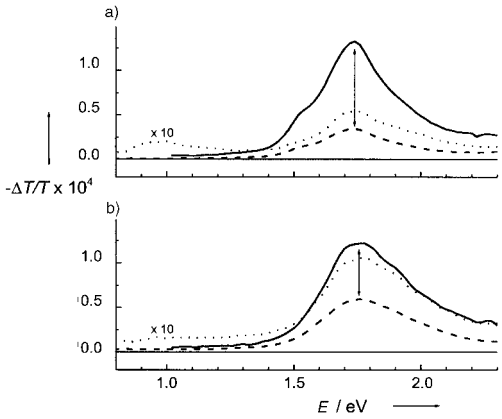

Figure 7. Photoinduced absorption spectra of **4TsC** (a) and **4TdC** (b) in toluene (----) and ODCB (••••, shown with tenfold magnification). λ_{ex} = 458 nm, 275 Hz, 25 mW, 298 K. The PIA spectra are compared to those of **C_{60}s** and **C_{60}d** (——), respectively.

for differences in optical density. When the dyads were dissolved in toluene identical spectra were obtained for excitation at 528 nm instead of 458 nm. In toluene, both dyads show a PIA band at 1.74 eV resulting from the C_{60} $T_n \leftarrow T_1$ transition. However, a distinct difference is seen for the intensity of the PIA bands of the dyads compared with **C_{60}s** and **C_{60}d**. For **4TsC**, the $C_{60}(T_n \leftarrow T_1)$ signal is reduced by a factor of three relative to **C_{60}s**, whereas for **4TdC** the signal intensity decreases by a factor of two compared to **C_{60}d**. These observations are in agreement with the proposed indirect electron transfer after full energy transfer from 4T(S_1) to $C_{60}(S_1)$, because the reduction of the triplet–triplet absorption equals the reduction in fullerene emission (Q_A(DA*)) in both dyads. The intramolecular charge-separated states $4T^{\bullet+}$–$C_{60}^{\bullet-}$ for **4TsC** and **4TdC** are not observed in these PIA spectra because the lifetimes are much shorter than the micro- to millisecond time domain. The almost identical quenching factors of the $C_{60}(S_0 \leftarrow S_1)$ PL and the $C_{60}(T_n \leftarrow T_1)$ PIA for **4TsC** and **4TdC** in toluene reveals, implicitly, that the decay of the intramolecular charge-separated state does not give rise to an additional population of the fullerene triplet state. We

  0947-6539/02/0823-5421 $ 20.00+.50/0

conclude that the intramolecular charge-separated state recombines directly to the ground state.

In ODCB, the PIA spectrum of **4TsC** shows very low intensity excited-state absorptions at 0.98 and 1.74 eV ($-\Delta T/T = 5 \times 10^{-6}$) as a result of a small extent of charge formation. The charges show bimolecular decay with lifetimes exceeding 10 ms. The more than 100 times lower signal intensity for **4TsC** in ODCB compared to the 1:1 molar mixture **4TP/C_{60}s** is attributed to fast recombination of opposite charges within the dyad to form the ground state. The presence of a small amount of long-lived charges is attributed to some intermolecular charge transfer. As a consequence of the low concentration of residual charges, the bimolecular recombination is reduced and lifetime increases.

In contrast to **4TsC**, the PIA spectrum of **4TdC** in ODCB resembles the spectrum of the triplet state of **C_{60}d** ($-\Delta T/T = 10^{-5}$) together with a very small additional feature at 0.98 eV ($-\Delta T/T \approx 5 \times 10^{-6}$). On changing the modulation frequency, the absorption band at 1.74 eV reveals the contributions of short-lived and long-lived components (Figure 8).[28] Note that the intensity of the 1.74 eV band is quenched compared to $C_{60}(T_n \leftarrow T_1)$ of pristine **C_{60}d**. Moreover, the intensity of the 0.98 eV signal is drastically reduced compared to 1:1 mixtures of **4TP/C_{60}d** in ODCB. These features point to rapid recombination of charges, which is indirectly reflected by the low intensity of $C_{60}(T_n \leftarrow T_1)$ absorption.

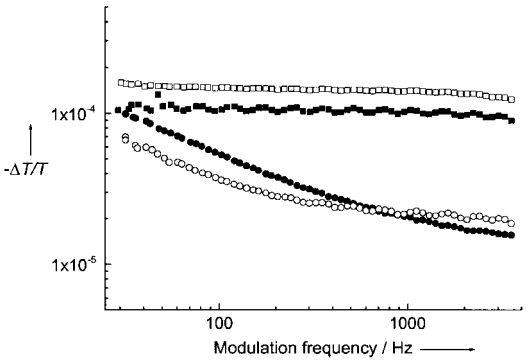

Figure 8. Frequency dependence of the 1.74 eV PIA signals of **4TsC** (filled symbols) and **4TdC** (open symbols) dyads in toluene (squares) and ODCB (circles). $\lambda = 458$ nm, 25 mW, 298 K.

The PIA spectra of the dyads show that, in ODCB, the free energy of the charge-separated state of **4TsC** is lower than that of **C_{60}s**(T_1), while the charge-separated states of **4TdC** and **C_{60}d**(T_1) are closer in energy than in the previous case.

In conclusion, the near-steady-state PIA experiments confirm the conclusions derived from the fluorescence studies. In addition, some information on the relative energetic positions of the charge-separated and triplet states was obtained. In the next section we focus on transient photoinduced absorption spectroscopy to gain more detailed insight into the rates of forward and backward electron transfer.

Transient photoinduced absorption spectroscopy: Both dyads were investigated in dilute solutions in toluene and ODCB ($(2-5) \times 10^{-4}$ M) by sub-picosecond photoinduced absorption spectroscopy. The dyads were photoexcited at 450 nm, and the change in transmission was monitored at 500, 880, and 1325 nm, respectively.

Stimulated emission of 4T: The deactivation of the 4T(S_1) state can be followed over time by probing the stimulated emission of the 4T chromophore at 500 nm. Due to the absence of direct charge transfer in toluene, the rate of energy transfer k_{ET} of both dyads can be obtained from the differential transmission dynamics at 500 nm. Pristine **4TP** shows the long-lived 4T($S_0 \leftarrow S_1$) signal with a time constant of 470 ps (Figure 9), similar to that obtained from time-resolved fluorescence spectroscopy. The flexible **4TsC** dyad shows a reduced transmission signal at 500 nm (Figure 9) that disappears within 2 ps, consistent with the time constant obtained from the quenching of the steady-state fluorescence. For **4TdC** no signal could be observed at 500 nm (Figure 9). This can be explained if the decay is faster than the resolution of our setup (ca. 300 fs). This corroborates with the value of less than 300 fs for singlet-energy transfer obtained from steady-state fluorescence spectroscopy.

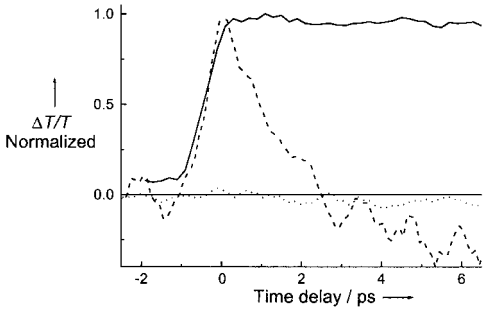

Figure 9. Differential transmission dynamics of the stimulated emission at 500 nm of the 4T chromophore for **4TP** (——), **4TsC** (- - - -), and **4TdC** (••••) in toluene at room temperature as function of the pump-probe delay after photoexcitation at 450 nm with a 150 fs pulse. Excitation wavelength $\lambda_{ex} =$ 450 nm.

Absorption of 4T radical cation: Next, the charge formation and recombination processes were studied in toluene and ODCB. To ensure that we are only looking at charged species, the dyads were probed at 1325 nm (0.94 eV), where the low-energy (LE) band of $4T^{\bullet+}$ is located (Figures 5 and 6). For **4TsC** in toluene, a low-intensity signal at 1325 nm was obtained, which reaches a maximum after 50 ps and decreases subsequently with a time constant of about 600 ps (Figure 10). In ODCB, the signal at 1325 nm attains its maximum intensity faster (<5 ps) and disappears with a time constant of about 350 ps (Figure 10).

The rise times of the 1325 nm signal (belonging to $4T^{\bullet+}$) for **4TsC** in toluene (50 ps) and ODCB (<5 ps) seem to be in conflict with k_{CS}^{i} and k_{CS}^{d} obtained from time-resolved PL and PL quenching data. However, both the low intensity of the signal and the short rise time can be explained when charge recombination is faster than charge formation. In that case, the amount of charge present is reduced dramatically. As a result, the decay of the signal at 1325 nm actually represents the amount of charged species formed with time, which

0947-6539/02/0823-5422 $ 20.00+.50/0 *Chem. Eur. J.* **2002**, *8*, No. 23

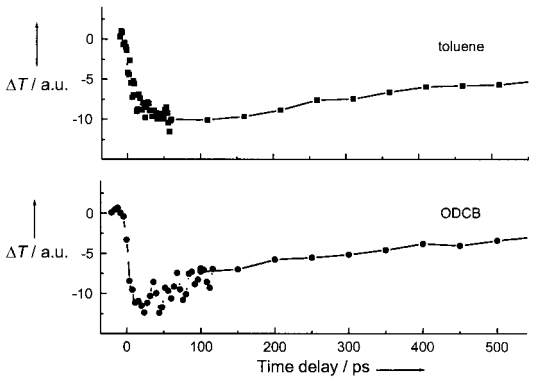

Figure 10. Differential transmission of the photoinduced absorption at 1325 nm of **4TsC** in toluene (top) and ODCB (bottom) as a function of the pump-probe time delay after photoexcitation at 450 nm with a 150 fs pulse.

state absorption at 880 nm. The fullerene reference compounds display a small signal at 880 nm with a time constant similar to the results obtained by Guldi et al.[16b] Besides the fullerene derivatives, pristine **4TP** was also probed at 880 nm. This revealed the presence of a strong excited state absorption, assigned to the $4T(S_n \leftarrow S_1)$ transition. The $4T(S_n \leftarrow S_1)$ signal at 880 nm decays with a time constant of 420 ps, comparable to the $4T(S_1)$ lifetime obtained by the temporal evolution of the 500 nm signal and from time-resolved PL spectroscopy. The **4TsC** dyad shows, both in toluene and in ODCB, an absorption signal that decays with two time constants (Figure 11 a and b). A short time constant of about 2 ps is attributed to the initial presence of a $4T(S_n \leftarrow S_1)$ absorption, which then turns into a $C_{60}(S_n \leftarrow S_1)$ excited-state absorption as a consequence of the fast energy-transfer

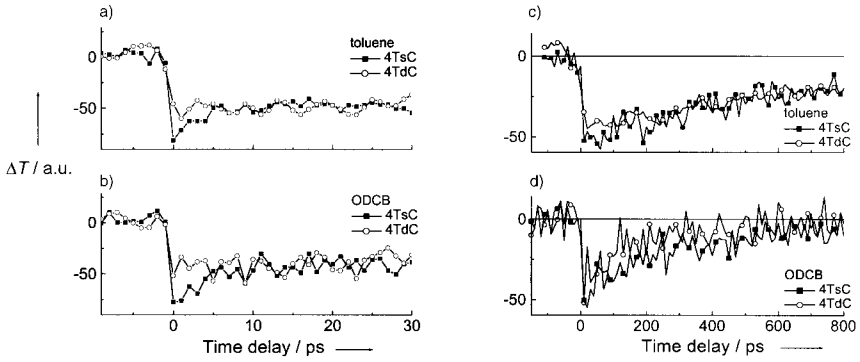

Figure 11. Differential transmission of the photoinduced absorption at 880 nm of **4TsC** (squares) and **4TdC** (circles) in toluene (a and c) and ODCB (b and d) as function of the pump-probe time delay following photoexcitation at 450 nm with a 150 fs pulse in the −10 to 30 ps (a and b) and −150 to 800 ps (c and d) time domains.

follows the decay of the $C_{60}(S_1)$ state of **4TsC** from which electron transfer takes place. In full agreement with this proposition, the lifetime of 610 ps for the $C_{60}(S_1)$ state of **4TsC** in toluene (Table 2) corresponds satisfactorily with the decay of the $4T^{\bullet+}$ signal at 1325 nm of 600 ps. The recombination rate can be estimated from the rise time of the 1325 nm signal, resulting in $k_{rec} = 6.7 \times 10^{10}\ s^{-1}$, which corresponds to a lifetime of about 15 ps. The explanation of the 1325 nm signal of $4T^{\bullet+}$–$C_{60}^{\bullet-}$ in ODCB is somewhat more difficult, as PL studies revealed the presence of two pathways (direct and indirect) for charge transfer with rates of $k_{CS}^{d} = 7.6 \times 10^{10}\ s^{-1}$ and $k_{CS}^{i} \approx 10^{9}\ s^{-1}$. Again, we envision the likelihood that recombination is faster than forward charge transfer to explain the low-intensity signal at 1325 nm. The decay at 1325 nm is in agreement with the lifetime of 350 ps for the $C_{60}(S_1)$ state of **4TsC**. The grow-in signal ($k > 5 \times 10^{11}\ s^{-1}$) can be attributed to a fast recombination process with a small contribution from the slower direct charge-transfer process, which is at least 6–7 times slower. Comparing recombination in toluene ($k_{rec} = 6.7 \times 10^{10}\ s^{-1}$, lifetime 15 ps) and ODCB ($k_{rec} \approx 5 \times 10^{11}\ s^{-1}$, lifetime 2 ps) we find that the rate of charge recombination is enhanced on increasing the polarity.

For **4TdC**, a very small signal at 1325 nm was detected, both in toluene and ODCB, which was not higher than approximately twice the noise level (detection limit: $\Delta T/T \approx 2 \times 10^{-4}$). These low intensities can be explained by charge-recombination processes that are faster than the charge-transfer processes, and this implies that in ODCB the rate constant for recombination is $k_{rec} > 10^{13}\ s^{-1}$, because fast direct charge transfer with $k_{CS}^{d} > 3 \times 10^{12}\ s^{-1}$ must be overcome.

C_{60} excited state absorption: To verify these results, the channel from which indirect charge transfer occurs, $C_{60}(S_1)$, was monitored in time by probing the $C_{60}(S_n \leftarrow S_1)$ excited process ($k_{ET} = 5 \times 10^{11}\ s^{-1}$) in both toluene and ODCB. The lifetime of the longer lived absorption is related to the rate of indirect charge transfer k_{CS}^{i}, and this absorption decays in toluene and ODCB with time constants of 710 and 360 ps, respectively. In both toluene and ODCB **4TdC** shows only one time constant (Figure 11), as the deactivation of $4T(S_1)$ to $C_{60}(S_1)$ occurs within the time resolution of our setup ($k_{ET} + k_{CS}^{d} > 3.3 \times 10^{12}\ s^{-1}$). In toluene, the decay of the $C_{60}(S_1)$ state of **4TdC** occurs with a time constant of 950 ps. In ODCB, the signal at 880 nm drops more rapidly to zero, with a time constant of 200 ps. The faster deactivation of the $C_{60}(S_1)$ state of **4TdC** in ODCB compared to the $C_{60}(S_1)$ state of **4TsC** is in agreement with the data on k_{CS}^{i} obtained from time-resolved PL and PL quenching.

According to differential transmission dynamics, both **4TsC** and **4TdC** display an ultrafast singlet-energy transfer from $4T(S_1)$ to $C_{60}(S_1)$ with rate constants of $k_{ET} = 5 \times 10^{11}\ s^{-1}$ and $k_{ET} > 3 \times 10^{12}\ s^{-1}$, respectively. Interestingly, the rate for charge recombination is higher than the rate of (in)direct charge formation. Although the rate for direct charge transfer cannot be derived from time-resolved photoinduced absorption, the rate for indirect charge transfer is obtained from the decay of both the 880 and 1325 nm signals and reveals the enhanced rate constant for **4TdC** in ODCB compared to **4TsC**.

In summary, the transient pump-probe experiments reveal that the deactivation of the $4T(S_1)$ state is very fast (< 2 ps).

  0947-6539/02/0823-5423 $ 20.00+.50/0

Electron transfer in the dyads occurs both by a direct mechanism from 4T(S_1) as well as via the C_{60}(S_1) state, which is formed by energy transfer. In the latter case the rate for charge separation is much slower. The fitting of the temporal absorption profiles reveals that the lifetime of the charge-separated state is very short, in the low picosecond range.

Energy of the charge-separated states and energy barriers for charge separation: To rationalize the energy- and electron-transfer reactions in apolar and polar solvents obtained from PL and PIA, we estimated the free energy for charge separation G_{CS} using the Weller equation [Eq. (6)].[20]

$$G_{CS} = e[E_{ox}(D) - E_{red}(A)] - \frac{e^2}{4\pi\varepsilon_0\varepsilon_s R_{cc}} - \frac{e^2}{8\pi\varepsilon_0}\cdot\left(\frac{1}{r^+}+\frac{1}{r^-}\right)\cdot\left(\frac{1}{\varepsilon_{ref}}-\frac{1}{\varepsilon_s}\right) \quad (6)$$

With the experimental data for the oxidation (E_{ox}) and reduction (E_{red}) potentials ($E_{1/2}$ is used in Eq. (6) rather than the peak potentials given in Table 1) measured in a solvent of relative permittivity ε_{ref}, together with estimated values for the radii of the charged molecules (r^+ and r^-) and the distance between the two charges R_{cc}, the Gibbs free energy of the charge-separated state G_{CS} can be calculated in solvents with varying polarity ε_s and compared to the excited state from which charge transfer occurs.

Energy of the charge-separated state: For **4TsC** and **4TdC**, E_{ox} and E_{red} were determined in dichloromethane ($\varepsilon_{ref} = 8.93$) by cyclic voltammetry (Table 1). The R_{cc} values for both dyads were determined by molecular modeling assuming localization of the charges at the center of quaterthiophene and fullerene moieties. This results for **4TdC** in $R_{cc} \approx 8.0$ Å. For **4TsC** two different R_{cc} values are used to account for the flexibility of the linker between the photoactive chromophores. The interchromophore distance for **4TsC** is set either at 8.0 Å, similar to **4TdC**, or to 20 Å for the extended conformation. For intermolecular charge transfer, the R_{cc} term was set to infinity. The radius of the $C_{60}^{\bullet-}$ radical anion was set to $r^- = 5.6$ Å, based on the density of C_{60}.[10a] The radius of the $4T^{\bullet+}$ radical cation (a simplification for a one dimensionally extended moiety) is obtained by calculating the van der Waals volume excluding the thioether side chains. From X-ray crystallographic studies on unsubstituted terthiophene[29] and sexithiophene,[30] the density ($\rho = 1.51$ g cm^{-3}) is known to be independent of the length, and hence the radii were determined from $r^+ = (3 \times 10^{24} M/4\pi\rho N_A)^{1/3}$ to be $r^+(3T) = 4.03$ Å and $r^+(6T) = 5.08$ Å. This approach results in a value of 4.43 Å for $r^+(4T)$. With these approximations, the free energy of intra- and intermolecular charge-separated states were estimated, and the relative ordering of the states is given in Figure 12 (see also Table 3). The energies of the singlet excited states from which intramolecular charge transfer can occur were obtained from fluorescence data and are 2.63, 1.78, and 1.75 eV for **4TP**(S_1), **C_{60}s**(S_1), and **C_{60}d**(S_1), respectively. Intermolecular charge transfer occurs from the triplet state of the fullerene, which has an energy of 1.50 eV, as inferred from phosphorescence data. For mixtures of **4TP** and **C_{60}s** or **C_{60}d** Equation (6) predicts that the charge-separated state cannot be obtained in toluene from the C_{60}(T_1) state. This is in agreement with the experimentally observed $C_{60}(T_n \leftarrow T_1)$ absorption in the PIA spectra (Figure 6). In the

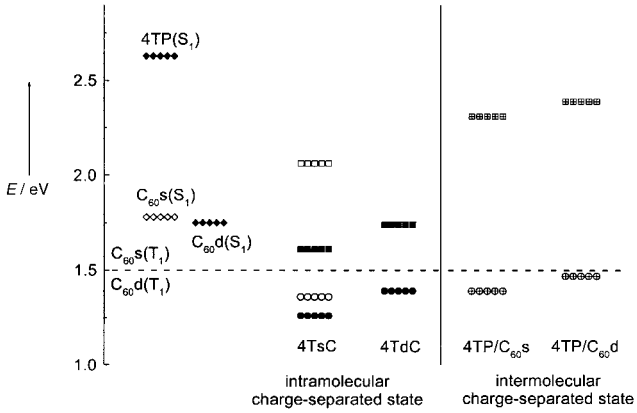

Figure 12. Free energy of intramolecular and intermolecular charge-separated states in **4TsC** and **4TdC** dyads and **4TP/C_{60}s** and **4TP/C_{60}d** mixtures in toluene (squares) and ODCB (circles) relative to the **4TP**(S_1), **C_{60}s**(S_1), and **C_{60}d**(S_1) singlet energies and the **C_{60}s**(T_1) and **C_{60}d**(T_1) triplet energies. Energies were calculated by using Equation (6) with $R_{cc} = 8.0$ Å (filled symbols), $R_{cc} = 20.0$ Å (open symbols), and $R_{cc} = \infty$ (crossed symbols).

Table 3. Free energies G_{CS} of the charge-separated states of **4TsC** and **4TdC** dyads and of **4TP/C_{60}s** and **4TP/C_{60}d** mixtures. Change in free energy ΔG_{CS} for charge separation relative to the singlet (S_1) and triplet (T_1) excited states of 4T and C_{60}. Energy barriers $\Delta G_{CS}^{\ddagger}$ for direct (4T(S_1)) and indirect (C_{60}(S_1)) charge transfer.

Sample	Solvent	R_{cc} [Å]	G_{CS}[a] [eV]	ΔG_{CS} 4T(S_1) [eV]	ΔG_{CS} C_{60}(S_1) [eV]	ΔG_{CS} C_{60}(T_1) [eV]	$\lambda_i + \lambda_s$[b] [eV]	$\Delta G_{CS}^{\ddagger}$[c] 4T(S_1) [eV]	$\Delta G_{CS}^{\ddagger}$[c] C_{60}(S_1) [eV]
4TsC	toluene	8.0	1.61	−1.02	−0.17	–	0.33	0.36	0.02
	ODCB	8.0	1.26	−1.37	−0.52	–	0.65	0.20	0.01
	toluene	20.0	2.06	−0.57	0.28	–	0.36	0.03	0.29
	ODCB	20.0	1.36	−1.27	−0.42	–	0.99	0.02	0.08
4TdC	toluene	8.0	1.74	−0.89	−0.01	–	0.33	0.24	0.08
	ODCB	8.0	1.39	−1.24	−0.36	–	0.65	0.14	0.03
4TP/C_{60}s	toluene	∞	2.31	–	–	0.81	0.38	–	–
	ODCB	∞	1.39	–	–	−0.11	1.21	–	–
4TP/C_{60}d	toluene	∞	2.39	–	–	0.89	0.38	–	–
	ODCB	∞	1.47	–	–	−0.03	1.21	–	–

[a] Calculated by using Equation (6). [b] Reorganization energy $\lambda_i + \lambda_s$ calculated from $\lambda_i = 0.3$ eV and λ_s from Equation (8). [c] Calculated from Equation (7).

0947-6539/02/0823-5424 $ 20.00+.50/0 *Chem. Eur. J.* **2002**, *8*, No. 23

more polar solvent ODCB, the free energy of the charge-separated state G_{CS} of both mixtures drops below the energy of $C_{60}(T_1)$. This is supported experimentally by the absorptions of a charge-separated state in the PIA experiment (Figure 6). For **4TP/C$_{60}$d**, the PIA spectrum shows the presence of both $C_{60}(T_1)$ and **4TP$^{\bullet+}$/C$_{60}$d$^{\bullet-}$**, in nice agreement with their almost equal energies (Figure 12 and Table 3). Increasing the polarity results in a further reduction of G_{CS} for both **4TP** mixtures. This was verified experimentally by using benzonitrile as solvent, in which the absorptions of the charge-separated states were obtained for both mixtures (Figure 6). In conclusion, G_{CS} as inferred from Equation (6) for the **4TP/C$_{60}$s** and **4TP/C$_{60}$d** mixtures is in full agreement with the experimental data for each of the three solvents studied.

For the dyads, the energy of the charge-separated state in toluene is lower than the **C$_{60}$s**(S_1) and **C$_{60}$d**(S_1) states when the center-to-center distance is small ($R_{cc} = 8.0$ Å). In accordance, a quenching of photoluminescence of the fullerene emission and a quenching of the fullerene triplet – triplet absorption are observed due to indirect charge transfer for both dyads in toluene. When the interchromophore distance is increased to 20 Å for **4TsC**, charge separation is strongly endergonic from the $C_{60}(S_1)$ state in toluene and unlikely to occur. This supports our assumption that for indirect charge transfer the flexible structure allows the donor and acceptor moieties to come close within the lifetime of the fullerene singlet excited state of about 1.5 ns.

Intramolecular charge transfer in both dyads in ODCB, as inferred from PIA spectra together with PL quenching and time-resolved PL data, is in accordance with the lower free energy of the charge-separated state (G_{CS}) compared to both the $4T(S_1)$ and $C_{60}(S_1)$ states, for both proximate and extended orientations of donor and acceptor.

Energy barriers for electron transfer: The direct electron transfer in ODCB and the absence thereof in toluene must be related to different activation barriers for direct electron transfer, because in both solvents a net gain in free energy would result.[31] The barrier for electron transfer $\Delta G^{\ddagger}$ depends on the change in Gibbs free energy for charge separation ΔG_{CS}, the internal reorganization energy λ_i, and the solvent reorganization energy λ_s. By using the Marcus equation, the activation barrier for direct $[\Delta G^{\ddagger}_{CS}(4T(S_1))]$ and indirect $[\Delta G^{\ddagger}_{CS}(C_{60}(S_1))]$ electron transfer can be calculated from the change in Gibbs free energy for charge separation from $\Delta G_{CS} = G_{CS} - E_{00}$, where E_{00} is the energy of the $4T(S_1)$ or $C_{60}(S_1)$ excited state, respectively [Eq. (7)].

$$\Delta G^{\ddagger}_{CS} = \frac{(\Delta G_{CS} + \lambda_i + \lambda_s)}{4(\lambda_i + \lambda_s)} \tag{7}$$

The internal reorganization energy is taken as $\lambda_i = 0.3$ eV based on the value determined by Verhoeven et al.[7a, 10a, 18b] from the charge-transfer absorption and emission spectra of the diethylaniline/C_{60} couple.[32] The solvent reorganization energy λ_s can be calculated from the Born – Hush approach [Eq. (8)][10a, 33]

$$\lambda_s = \frac{e^2}{4\pi\varepsilon_0}\left[\frac{1}{2}\left(\frac{1}{r^+} + \frac{1}{r^-}\right) - \frac{1}{R_{cc}}\right]\left(\frac{1}{n^2} - \frac{1}{\varepsilon_s}\right) \tag{8}$$

where n is the refractive index of the solvent. Comparison of the total reorganization energy ($\lambda = \lambda_s + \lambda_i$) with the change in free energy for charge separation ΔG_{CS} (Table 3) shows that in these dyads indirect photoinduced electron transfer [i.e., from $C_{60}(S_1)$] occurs within the "normal" Marcus region ($\lambda > -\Delta G_{CS}$), while the direct electron transfer [i.e., from $4T(S_1)$] occurs in the Marcus "inverted" region ($\lambda < -\Delta G_{CS}$). The direct electron transfer is situated rather far in the inverted region as a consequence of the high energy of the S_1 state of **4TP**. The barriers for indirect charge transfer $[\Delta G^{\ddagger}_{CS}(C_{60}(S_1))]$ in both dyads are low (< 0.1 eV) in both solvents. Hence, indirect charge transfer within the normal region can occur for both dyads in both solvents. The barriers for direct charge transfer $[\Delta G^{\ddagger}_{CS}(4T(S_1))]$ are significantly higher in toluene than in ODCB for both dyad molecules. Consequently, a direct electron transfer from the $4T(S_1)$ state is hampered in toluene, because the activation barrier for charge transfer in the inverted region is too high. In ODCB, the barrier for direct charge transfer is apparently sufficiently reduced.

For the flexible dyad, the distance between the chromophores dramatically influences the activation barrier for direct and indirect charge transfer. At short interchromophore distance (8 Å) indirect charge transfer occurs in both toluene and ODCB, as the barrier for indirect charge transfer $[\Delta G^{\ddagger}_{CS}(C_{60}(S_1)]$ is sufficiently low, while the barrier for direct charge transfer $[\Delta G^{\ddagger}_{CS}(4T(S_1)]$ is rather high. Increasing the center-to-center distance lowers the barrier, so that direct charge transfer can occur. However, with increasing distance the electronic coupling V between donor and acceptor in the excited state, which according to Equation (9) determines the rate constant for nonadiabatic charge separation together with $\Delta G^{\ddagger}_{CS}$ and λ, is dramatically reduced.

$$k_{CS} = \left(\frac{4\pi^3}{h^2\lambda k_B T}\right)^{1/2} V^2 \exp\left(\frac{-\Delta G^{\ddagger}_{CS}}{k_B T}\right) \tag{9}$$

It is important to note that V is not only determined by the distance. More specifically, V depends on the overlap of the wavefunctions of the donor and acceptor in the excited state. Hence, V will strongly depend on the mutual orientation and the flexibility or fixation of the two chromophores in space. These factors are also important when addressing the question whether through-space charge separation is more efficient than through-bond charge separation. The experiments on **4TsC** and **4TdC** suggest that the through-space process is preferred because the chromophores are linked by the same saturated spacers. For a through-space charge transfer, the overlap of donor and acceptor is of course essential, even more so than a simple parameter as the distance.

Conclusion

Singly or doubly connected quaterthiophene – fullerene dyads show both energy and electron transfer in toluene and ODCB. Spectral evidence for charge formation within these dyads was obtained by photoinduced absorption spectroscopy. In toluene, the charge-separated state is reached in both cases by indirect charge transfer with rate constants on the order of

  0947-6539/02/0823-5425 $ 20.00+.50/0

$10^9\ s^{-1}$ following a singlet-energy transfer reaction from $4T(S_1)$ to $C_{60}(S_1)$. No direct charge transfer from $4T(S_1)$ is observed in toluene, as the barrier for this process is insuperable. In ODCB, direct charge transfer occurs from $4T(S_1)$ in addition to the indirect pathway, and for both dyads its rate is competive with the fast energy-transfer processes. Direct electron transfer in ODCB is a consequence of the reduced activation energy barrier for this process compared to toluene. The rate constants of direct electron transfer and energy transfer for the geometrically constrained dyad **4TdC** are one order of magnitude larger than for the flexible **4TsC**. This tenfold increase indicates that the constraints imposed on the orientation of the chromophores in the **4TdC** dyad result in stronger interactions between the excited states of the 4T and C_{60} chromophores. The Gibbs free energy for charge separation in solution, expressed by the Weller equation, fully supports and explains the experimental data of both dyads in solvents of different polarity.

In solution, the rate constants for the recombination of the geminate pair of charges in **4TsC** and **4TdC** are higher than the rate of their formation, as was inferred from fitting the transient profile of the $4T^{\bullet+}$ absorption by using the forward electron-transfer rates obtained from photoluminescence spectroscopy. This fast recombination of opposite charges contrasts with porphyrin – C_{60} dyads, for which lifetimes of the charge-separated state in the range of 10 – 100 ps were reported.[11] Because the recombination is deeply in the inverted region, the origin of the fast recombination cannot be explained by Marcus theory. Hence, further studies are required to understand the recombination of charges in these face-to-face complexes.

Of course, a fast intramolecular recombination reaction is not beneficial for a good photovoltaic cell. However, the near-steady-state PIA experiments show that, in contrast to the fast recombination in solution, the lifetime of some charges created in the solid state extends into the micro- to millisecond time domain. This much longer lifetime in the solid state is attributed to positive and negative charges that avoid geminate (intramolecular) recombination and migrate to adjacent dyad molecules in the film, in agreement with previous reports.[3c] Future investigations will focus on establishing the discrimination between recombination and charge migration in more detail.

In conclusion, the faster intramolecular energy transfer and electron transfer in **4TdC** compared to **4TsC** results from the imposed face-to-face orientation of the donor and acceptor chromophores. We conjecture that the high rate of electron transfer observed in solid-state mixtures of conjugated polymers and fullerenes[2, 3] is caused by a similar face-to-face orientation of the two chromophores formed spontaneously in these blends.

Experimental Section

Materials: 3-(2-Cyanoethylsulfanyl)thiophene (**5**) and 5,5′-bis(tributylstannyl)-2,2′-bithiophene (**2**) were prepared according to known procedures.

2-Bromo-3-(2-cyanoethylsulfanyl)thiophene (4): A solution of *N*-bromosuccinimide (1.05 g, 5.92 mmol) in DMF (10 mL) was added dropwise to a solution of **5** (1.0 g, 5.92 mmol) in DMF (10 mL) under N_2 at 0 °C in the absence of light. The mixture was stirred for 4 h at room temperature, concentrated in vacuo, and the residue diluted with CH_2Cl_2 (150 mL). The organic phase was washed with water, dried over Na_2SO_4, evaporated in vacuo, and purified by chromatography on silica gel (CH_2Cl_2/petroleum ether (PE) 1:1) to give a white solid (1.33 g, 90 %). M.p. 40 – 41 °C; ^{1}H NMR ($CDCl_3$): $\delta = 2.57$ (t, 2H, $^3J = 7.5$ Hz), 3.05 (t, 2H, $^3J = 7.5$ Hz), 7.00 (d, 1H, $^3J = 5.7$ Hz), 7.32 (d, 1H, $^3J = 5.7$ Hz); ^{13}C NMR ($CDCl_3$): $\delta = 18.6$, 30.8, 117.8, 118.5, 126.8, 129.6, 131.5; IR (KBr): $\tilde{\nu} = 2246\ cm^{-1}$ (CN); elemental analysis (%) calcd for: C 33.88, H 2.44, S 25.84, N 5.64; found: C 33.88, H 2.38, S 25.54, N 5.62.

3,3‴-Bis(2-cyanoethylsulfanyl)-2,2′:5′,2″:5″,2‴-quaterthiophene (1): A mixture of **4** (0.5 g, 2 mmol), 5,5′-bis(tributylstannyl)-2,2′-bithiophene (**2**; 0.57 g, 0.8 mmol), and $[Pd(PPh_3)_4]$ (116 mg, 5 mol %) in anhydrous toluene (15 mL) was refluxed overnight under an N_2 atmosphere. After cooling to room temperature, an orange precipitate was recovered and washed several times with pentane. Chromatography on silica gel (CH_2Cl_2) gave a powder (0.32 g, 85 %), which was then recrystallized from CH_2Cl_2/toluene 1:1 to give pure **1** (0.28 g). M.p. 149 – 150 °C; UV/Vis (CH_2Cl_2): $\lambda = 404$ nm ($\lg \varepsilon = 4.40$); ^{1}H NMR ($CDCl_3$): $\delta = 2.57$ (t, 4H, $^3J = 7.3$ Hz), 3.05 (t, 4H, $^3J = 7.3$ Hz), 7.08 (d, 2H, $^3J = 5.2$ Hz), 7.18 (d , 2H, $^3J = 4.2$ Hz), 7.24 (d, 2H, $^3J = 5.2$ Hz), 7.33 (d, 2H, $^3J = 4.2$ Hz); ^{13}C NMR ($CDCl_3$): $\delta = 18.48$, 31.72, 117.85, 123.88, 123.97, 124.00, 127.71, 133.48, 133.89, 137.93, 139.47; IR (KBr): $\tilde{\nu} = 2246\ cm^{-1}$; MS (70 eV, EI): *m*/*z* (%): 500 [M^+] (63), 447 (31), 394 (29), 360 (43), 83 (42), 69 (75), 57 (87), 55 (100); HRMS calcd for $C_{22}H_{16}N_2S_6$: 499.963779; found: 499.960226; elemental analysis (%) calcd for: C 52.77, H 3.22, S 38.41, N 5.59; found: C 52.82, H 3.24, S 37.74, N 5.49.

3-(2-Cyanoethylsulfanyl)-3‴-(pentylsulfanyl)-2,2′:5′,2″:5″,2‴-quaterthiophene (7): Under inert atmosphere a solution of cesium hydroxide (134 mg, 1 equiv) in degassed methanol (5 mL) was added dropwise to a solution of **1** (400 mg, 0.8 mmol.) in degassed DMF (30 mL). The mixture was stirred for 1 h at room temperature, and 1-iodopentane (60 mg, 4 equiv) added. After 1 h of stirring at room temperature and solvent removal, the residue was dissolved in dichloromethane. The solution was washed with water, dried over Na_2SO_4, concentrated, and purified by chromatography on silica gel (CH_2Cl_2/PE 4:1) to give an orange oil (215 mg, 52 %). ^{1}H NMR ($CDCl_3$): $\delta = 7.32$ (d, 1H, $^3J = 3.9$ Hz), 7.30 (d, 1H, $^3J = 3.9$ Hz), 7.23 (d, 1H, $^3J = 5.3$ Hz), 7.19 (d, 1H, $^3J = 5.3$ Hz), 7.16 (d, 1H, $^3J = 3.9$ Hz), 7.15 (d, 1H, $^3J = 3.9$ Hz), 7.08 (d, 1H, $^3J = 5.2$ Hz), 7.04 (d, 1H, $^3J = 5.2$ Hz), 3.04 (t, 2H, $^3J = 7.3$ Hz, CH_2S), 2.87 (t, 2H, $^3J = 7.4$ Hz, CH_2S), 2.56 (t, 2H, $^3J = 7.3$ Hz, CH_2CN), 1.62 (qu, 2H, $^3J = 7.4$ Hz), 1.40 – 1.34 (m, 2H), 1.32 – 1.27 (m, 2H), 0.87 (t, 3H, $^3J = 7.3$ Hz, CH_3); ^{13}C NMR ($CDCl_3$): $\delta = 139.6$, 138.4, 137.0, 135.6, 135.1, 133.5, 132.2, 128.3, 127.7, 126.9, 123.8 (2C), 123.5, 123.3, 117.8, 36.2, 31.7, 30.9, 29.3, 22.2, 18.5, 13.9; MS (MALDI): *m*/*z*: 517 [M^+], 463; IR (KBr): $\tilde{\nu} = 2246\ cm^{-1}$ (CN).

3,3‴-Bis-(pentylsulfanyl)-2,2′:5′,2″:5″,2‴-quaterthiophene (4TP): This compound resulting from the deprotection of two thiolate groups was isolated (70 mg, 16 %) during the preparation of **7**. The pure compound was obtained as an orange oil after chromatography on silica gel (CH_2Cl_2/PE 3:7). ^{1}H NMR ($CDCl_3$): $\delta = 7.29$ (d, 2H, $^3J = 3.8$ Hz), 7.18 (d, 2H, $^3J = 5.3$ Hz), 7.15 (d, 2H, $^3J = 3.8$ Hz), 7.04 (d, 2H, $^3J = 5.3$ Hz), 2.86 (t, 4H, $^3J = 7.4$ Hz, CH_2S), 1.62 (qu, 4H, $^3J = 7.4$ Hz), 1.46 – 1.19 (m, 8H), 0.87 (t, 6H, $^3J = 7.2$ Hz, CH_3); ^{13}C NMR ($CDCl_3$): $\delta = 137.5$, 135.8, 134.7, 132.3, 128.0, 126.8, 123.5, 123.1, 36.2, 30.9, 29.3, 22.2, 13.9; MS (MALDI): *m*/*z*: 534 [M^+], 463; HMRS (ESI +): calcd for $C_{26}H_{30}S_6$: 534.0672; found: 534.0652.

3-(2-Hydroxyethylsulfanyl)-3‴-(pentylsulfanyl)-2,2′:5′,2″:5″,2‴-quaterthiophene (9): This compound was obtained from compound **7** according to the procedure described for **7** by using CsOH (74 mg, 1 equiv), **7** (200 mg, 0.4 mmol), and 2-bromoethanol (200 mg, 4 equiv). The pure compound was obtained as an orange oil (110 mg, 56 %) after chromatography on silica gel (CH_2Cl_2/PE 9:1). ^{1}H NMR ($CDCl_3$): $\delta = 7.31$ (d, 1H, $^3J = 3.8$ Hz), 7.29 (d, 1H, $^3J = 3.8$ Hz), 7.20 (d, 1H, $^3J = 5.3$ Hz), 7.17 (d, 1H, $^3J = 5.1$ Hz), 7.15 (d, 2H, $^3J = 3.8$ Hz), 7.06 (d, 1H, $^3J = 5.3$ Hz), 7.04 (d, 1H, $^3J = 5.1$ Hz), 3.67 (q, 2H, $^3J = 6.0$ Hz, CH_2O), 3.02 (t, 2H, $^3J = 6.0$ Hz, CH_2S), 2.86 (t, 2H, $^3J = 7.3$ Hz, CH_2S), 2.03 (t, 1H, $^3J = 6.0$ Hz, OH); 1.62 (qui, 2H, $^3J = 7.6$ Hz); 1.45 – 1.24 (m, 4H); 0.87 (t, 3H, $^3J = 7.0$ Hz, CH_3); ^{13}C NMR ($CDCl_3$): $\delta = 138.0$, 137.8, 137.1, 135.7, 135.0, 134.0, 132.9, 132.3, 128.2, 127.4, 126.8, 125.7, 123.7, 123.6, 123.5, 123.2, 60.6, 39.6, 36.2, 30.9, 29.3, 22.2, 13.9; MS (MALDI): *m*/*z*: 508 [M^+], 463; IR (KBr): $\tilde{\nu} = 3370\ cm^{-1}$ (OH); UV/Vis (CH_2Cl_2): $\lambda = 403$ nm ($\lg \varepsilon = 4.37$).

0947-6539/02/0823-5426 $ 20.00+.50/0 *Chem. Eur. J.* **2002**, *8*, No. 23

3,3‴-Bis-(2-hydroxyethylsulfanyl)-2,2′:5′,2″:5″,2‴-quaterthiophene (8): This compound was prepared using the method described for **9**, from **1** (100 mg, 0.2 mmol), CsOH (70 mg, 2.1 equiv), and 2-bromoethanol (300 mg, 6 equiv). Chromatography on silica gel (CH_2Cl_2/AcOEt 8.5:1.5) gave a yellow solid (50 mg, 52 %). M.p. 70 – 72 °C; ^{1}H NMR ($CDCl_3$): $\delta =$ 7.31 (d, 2H, $^3J = 3.9$Hz), 7.21 (d, 2H, $^3J = 5.2$Hz), 7.16 (d, 2H, $^3J = 3.9$ Hz), 7.07 (d, 2H, $^3J = 5.2$ Hz), 3.68 (m, 4H, CH_2O), 3.03 (t, 4H, $^3J = 5.8$ Hz, CH_2S), 2.07 (t, 2H, $^3J = 6.4$ Hz, OH); ^{13}C NMR ($CDCl_3$): $\delta = 137.7$ (2C), 137.6 (2C), 134.3 (2C), 132.9 (2C), 127.4 (2C), 125.9 (2C), 123.8 (2C), 123.7 (2C), 60.7 (2C), 39.6 (2C); MS (MALDI): m/z: 482 [M^+], 436.

3-(Ethoxycarbonylacetoxyethylsulfanyl)-3‴-(pentylsulfanyl)-2,2′:5′,2″:5″,2‴-quaterthiophene (10): A solution of **9** (100 mg, 0.20 mmol), 3-chloro-3-ethyloxopropanoate (0.16 mL, 6 equiv) and pyridine (0.10 mL, 6 equiv) in CH_2Cl_2 (30 mL) was heated under reflux for 12 h under inert atmosphere. After cooling to room temperature and addition of CH_2Cl_2 (50 mL), the mixture was washed successively with aqueous HCl (0.5 N), saturated Na_2CO_3, and water. The organic phase was dried over Na_2SO_4, concentrated, and purified by chromatography on silica gel (CH_2Cl_2/PE 9:1) to give an orange oil (103 mg,84 %). ^{1}H NMR ($CDCl_3$): $\delta = 7.30$ (d, 1H, $^3J = 4.1$ Hz), 7.29 (d, 1H, $^3J = 4.7$ Hz), 7.20 (d, 1H, $^3J = 5.5$ Hz), 7.18 (d, 1H, $^3J = 5.5$ Hz), 7.16 (d, 1H, $^3J = 3.7$ Hz), 7.15 (d, H, $^3J = 3.7$ Hz), 7.07 (d, 1H, $^3J = 5.3$ Hz), 7.04 (d, 1H, $^3J = 5.3$ Hz), 4.27 (t, 2H, $^3J = 6.8$ Hz, CH_2O), 4.19 (q, 2H, $^3J = 7.1$ Hz, CH_2O), 3.33 (s, 2H), 3.07 (t, 2H, $^3J = 6.8$ Hz, CH_2S), 2.86 (t, 2H, $^3J = 7.4$ Hz, CH_2S), 1.62 (qui, 2H, $^3J = 7.6$ Hz), 1.42 – 1.35 (m, 2H), 1.32 – 1.24 (m, 5H), 0.87 (t, 3H, $^3J = 7.2$ Hz, CH_3); ^{13}C NMR ($CDCl_3$): $\delta = 166.3$, 166.2, 138.0, 137.8, 137.2, 135.7, 134.9, 134.1, 133.0, 132.3, 128.2, 127.3, 126.8, 125.6, 124.4, 123.7, 123.5, 123.2, 63.9, 61.6, 41.4, 36.2, 34.2, 30.9, 29.3, 22.2, 14.1, 13.9; UV/Vis (CH_2Cl_2): $\lambda = 403$ nm ($\lg \varepsilon = 4.32$); IR (KBr): $\tilde{\nu} = 1752$, 1736 cm^{-1} (C=O); MS (MALDI): m/z: 622 [M^+], 391.

3,3‴-Bis(ethoxycarbonylacetoxyethylsulfanyl)-2,2′:5′,2″:5″,2‴-quaterthiophene (11): This compound was prepared using the procedure already described for **10**, from **8** (200 mg, 0.42 mmol), 3-chloro-3-ethyloxopropanoate (0.25 mL 4 equiv), and pyridine (0.14 mL, 4 equiv) in CH_2Cl_2 (50 mL). Chromatography on silica gel (CH_2Cl_2/AcOEt 9.5:0.5) gave an orange solid (215 mg, 73 %). M.p. 41 – 43 °C; ^{1}H NMR ($CDCl_3$): $\delta = 7.30$ (d, 2H, $^3J = 3.9$ Hz), 7.20 (d, 2H, $^3J = 5.3$ Hz), 7.16 (d, 2H, $^3J = 3.9$ Hz), 7.08 (d, 2H, $^3J = 5.3$ Hz), 4.27 (t, 4H, $^3J = 6.9$ Hz, O-CH_2), 4.19 (q, 4H, $^3J = 7.1$Hz, O-CH_2), 3.32 (s, 4H), 3.07 (t, 4H, $^3J = 6.9$ Hz, CH_2S), 1.27 (t, 6H, $^3J =$ 7.1 Hz, CH_3); ^{13}C NMR ($CDCl_3$): $\delta = 166.3$ (4C), 137.7 (2C), 134.4 (2C), 133.0 (2C), 127.4 (2C), 125.7 (2C), 123.0 (6C), 63.9 (2C), 61.6 (2C), 41.4 (2C), 34.2 (2C), 14.0(2C); IR (KBr): $\tilde{\nu} = 1750$, 1728 cm^{-1} (C=O); UV/Vis (CH_2Cl_2): $\lambda = 404$ nm ($\lg \varepsilon = 4.44$); MS (MALDI): m/z: 710 [M^+], 391.

Compound 4TsC: A solution of C_{60} (82 mg 1.3 equiv), DBU (0.04 mL, 3 equiv), iodine (73 mg, 2.5 equiv), and **10** (93 mg, 0.15 mmol) in anhydrous toluene (160 mL) was stirred at room temperature under inert atmosphere for 12 h. After addition of water (200 mL), the organic phase was separated, and the aqueous phase extracted with dichloromethane. The organic phase was washed with water, dried over Na_2SO_4, and concentrated, and the residue was purified by chromatography on silica gel (CH_2Cl_2/PE 3:2) to give a dark solid (60 mg, 42 %). M.p. 65 – 67 °C; ^{1}H NMR (C_6D_6/CS_2): $\delta = 7.16$ (d, 1H, $^3J = 3.9$ Hz), 7.07 (d, 1H, $^3J = 3.9$ Hz), 7.06 (d, 1H, $^3J = 5.3$ Hz), 6.99 (d, 1H, $^3J = 4.9$ Hz), 6.98 (d, 1H, $^3J = 4.9$ Hz), 6.96 (d, H, $^3J = 3.9$ Hz), 6.95 (d, 1H, $^3J = 3.9$ Hz), 6.83 (d, 1H, $^3J = 5.3$ Hz), 4.42 – 4.34 (m, 4H, CH_2O), 3.07 (t, 2H, $^3J = 6.8$ Hz, CH_2S), 2.70 (t, 2H, $^3J =$ 7.4 Hz, CH_2S), 1.50 (qui, 2H, $^3J = 7.5$ Hz), 1.38 – 1.30 (m, 3H), 1.30 – 1.15 (m, 4H), 0.80 (t, 3H, $^3J = 7.2$ Hz, CH_3); MS (MALDI): m/z: 1340 [M^+], 463; HRMS calcd for $C_{88}H_{28}O_4S_6$: 1340.0311; found: 1340.0291. elemental analysis (%) calcd for: C 78.80, H 2.11, O 4.77, S 14.62; found: C 78.71, H 2.49, O 4.53, S 14.32; UV/Vis (CH_2Cl_2): $\lambda = 403$ ($\lg \varepsilon = 4.45$), 327 (4.60), 257 nm (5.06); IR (KBr): $\tilde{\nu} = 1744$, 1721 (C=O), 1231, 526 cm^{-1}.

Compound 4TdC: This compound was prepared using the method described for **4TsC** from C_{60} (138 mg, 0.19 mmol), **11**, (150 mg, 1.1 equiv), DBU (0.12 mL, 6 equiv), and iodine (242 mg, 5 equiv) in anhydrous toluene (250 mL). Chromatography on silica gel (CH_2Cl_2/PE 7:3) gave a dark solid (95 mg, 35 %) consisting of a mixture of several isomers. M.p. 160 – 164 °C; ^{1}H NMR ($CDCl_3$): $\delta = 7.32 – 6.85$ (m, 8H_{thio}), 4.77 – 4.35 (m, 8H, OCH_2), 3.36 – 3.05 (m, 4H, SCH_2), 1.61 – 1.36 (m, 6H, CH_3); IR (KBr): $\tilde{\nu} = 1746$, 1721 (C=O), 1231, 525 cm^{-1}; UV/Vis (CH_2Cl_2): $\lambda = 404$ ($\lg \varepsilon =$ 4.33), 250 nm (4.96); MS (MALDI): m/z: 1426 [M^+]; HRMS (ESI +): calcd for $C_{90}H_{26}O_8S_6$: 1425.9952; found: 1425.9926; elemental analysis (%) found (calcd): C (74.74) 74.41, H (1.84) 1.49, S (13.45) 12.89.

C_{60}s and C_{60}d: These compounds were prepared using the procedure described for **4TsC** from C_{60} (200 mg, 0.28 mmol), ethyl bromomalonate (100 mg, 1.5 equiv), and DBU (126 mg, 3 equiv) in anhydrous toluene (400 mL). Chromatography on silica gel (CH_2Cl_2/PE 1:1) gave the mono-adduct **C_{60}s** (65 mg, 27 %) and the bis-adduct (50 mg, 17.5 %) **C_{60}d** as a mixture of isomers. **C_{60}s**: m.p. > 250 °C; ^{1}H NMR ($CDCl_3$): $\delta = 4.35$ (q, 4H, $^3J = 7.1$ Hz, OCH_2), 1.35 (t, 6H, $^3J = 7.1$ Hz, CH_3); MS (MALDI): m/z: 878 [M^+], 720; IR (KBr): $\tilde{\nu} = 1746$ (C=O) 1236, 526 cm^{-1}; UV/Vis (CH_2Cl_2): $\lambda = 425$, 326, 257 nm. **C_{60}d**: m.p. 122 – 124 °C, ^{1}H NMR ($CDCl_3$): $\delta = 4.65 –$ 4.35 (m, 8H, O-CH_2), 1.65 – 1.35 (m, 12H, CH_3); MS (MALDI): m/z: 1036 [M^+], 878, 720; IR (KBr): $\tilde{\nu} = 1746$ (C=O), 1236, 526 cm^{-1}; UV/Vis (CH_2Cl_2): $\lambda = 422$, 250 nm.

Electrochemistry: Electrochemical measurements were carried out with a PAR 273 Potentiostat-Galvanostat in a three-electrode, single-compartment cell equipped with platinum microelectrodes of 7.85×10^{-3} cm^2 area, a platinum wire counterelectrode, and an Ag/AgCl reference electrode. Experiments were performed in dichloromethane (HPLC grade) containing 0.20 M Bu_4NPF_6. Solutions were deaerated by argon bubbling prior to all experiments, which were run under an argon atmosphere.

Absorption and fluorescence spectroscopy: UV/Vis absorption and fluorescence spectra were recorded on a Perkin – Elmer Lambda 40 spectrometer and an Edinburgh Instruments FS920 double-monochromator luminescence spectrometer using a Peltier-cooled red-sensitive photomultiplier, respectively. All UV/Vis and fluorescence measurements were carried out in 10 mm quartz cells. All measurements were carried out at room temperature unless indicated otherwise. Spectra were not corrected for the Raman scattering of the solvent. Solvents for absorption and fluorescence measurements were used as received.

Time-correlated single-photon counting: Time-correlated single-photon counting fluorescence studies were performed using an Edinburgh Instruments LifeSpec-PS spectrometer. The LifeSpec-PS comprises a 400 nm picosecond laser (PicoQuant PDL 800B) operated at 2.5 MHz and a Peltier-cooled Hamamatsu microchannel plate photomultiplier (R3809U-50). Lifetimes were determined from the data by using the Edinburgh Instruments software package.

Near-steady-state PIA: Solutions containing 2×10^{-4} M of each compound were prepared in a nitrogen-filled glove box in order to exclude interference of oxygen during measurements. The PIA spectra were recorded between 0.5 and 3.0 eV by exciting with a mechanically modulated cw Ar ion laser ($\lambda = 458$ or 528 nm, 275 Hz) pump beam and monitoring the resulting change in transmission of a tungsten halogen probe light through the sample (ΔT) with a phase-sensitive lock-in amplifier after dispersion by a grating monochromator and detection by Si, InGaAs, and cooled InSb detectors. The pump power incident on the sample was typically 25 mW with a beam diameter of 2 mm. The PIA ($-\Delta T/T \approx \Delta \alpha d$) was directly calculated from the change in transmission after correction for the photoluminescence, which was recorded in a separate experiment. Photoinduced absorption spectra and photoluminescence spectra were recorded with the pump beam in a direction almost parallel to the direction of the probe beam. The solutions were studied in a 1 mm near-IR-grade quartz cell at room temperature. Solvents for PIA measurements were distilled under nitrogen before use. The solid-state measurements were performed on films drop cast from chloroform solution onto a quartz substrate and held at 80 K in an Oxford continuous-flow cryostat.

Transient subpicosecond photoinduced absorption: The femtosecond laser system used for pump-probe experiments consists of an amplified Ti/sapphire laser (Spectra Physics Hurricane). The single pulses from a cw mode-locked Ti/sapphire laser were amplified by an Nd/YLF laser by using chirped pulse amplification, providing 150 fs pulses at 800 nm with an energy of 750 μJ and a repetition rate of 1 kHz. The pump pulses at 450 nm were created by optical parametric amplification (OPA) of the 800 nm pulse by a BBO crystal into infrared pulses, which were then twice frequency-doubled by BBO crystals. The probe beam was generated in a separate optical parametric amplification setup, in which the 500, 880, and 1325 nm pulses were created. The pump beam was focused to a spot size of about 1 mm^2 with an excitation flux of 1 mJ cm^{-2} per pulse. For the 880 nm and 1325 nm pulses a RG 850 nm cutoff filter was used to avoid contributions of residual probe light (800 nm) from the OPA. The probe beam was reduced in intensity compared to the pump beam by using

neutral-density filters of OD = 2. The pump beam was linearly polarized at the magic angle of 54.7° with respect to the probe, to cancel out orientation effects in the measured dynamics. The temporal evolution of the differential transmission was recorded by an InGaAs detector by a standard lock-in technique at 500 Hz. Solutions on the order of $2-5\times10^{-4}$ M were excited at 450 nm to provide primarily excitation of the 4T part within the dyad molecules.

Acknowledgement

This work was financially supported by the E.E.T. program (EETK97115) and by the Council for Chemical Sciences of the Netherlands Organization for Scientific Research (CW-NWO) and the Eindhoven University of Technology in the PIONIER program (98400). The research of S.C.J.M. has been made possible by a fellowship of the Royal Netherlands Academy of Arts and Sciences.

[1] a) G. Yu, J. Gao, J. C. Hummelen, F. Wudl, A. J. Heeger, *Science* **1995**, *270*, 1789; b) G. Yu, A. J. Heeger, *J. Appl. Phys.* **1995**, *78*, 4510; c) S. E. Shaheen, J. C. Brabec, F. Padinger, T. Fromherz, J. C. Hummelen, N. S. Sariciftci, *Appl. Phys. Lett.* **2001**, *78*, 841.

[2] C. J. Brabec, G. Zerza, G. Cerullo, S. De Silvestri, S. Luzzati, J. C. Hummelen, N. S. Sariciftci, *Chem. Phys. Lett.* **2001**, *340*, 232.

[3] a) N. S. Sariciftci, L. Smilowitz, A. J. Heeger, F Wudl, *Science* **1992**, *258*, 1474; b) L. Smilowitz, N. S. Sariciftci, R. Wu, C Gettinger, A. J. Heeger, F. Wudl, *Phys. Rev. B* **1993**, *47*, 13835; c) S. C. J. Meskers, P. A. van Hal, A. J. H. Spiering, J. C. Hummelen, A. F. G. van der Meer, R. A. J. Janssen, *Phys. Rev. B* **2000**, *61*, 9917.

[4] J. J. Apperloo, C. Martineau, P. A. van Hal, J. Roncali, R. A. J. Janssen, *J. Phys. Chem. A* **2002**, *106*, 21.

[5] a) P. A. van Hal, R. A. J. Janssen, G. Lanzani, G. Cerullo, M. Zavelani-Rossi, S. De Silvestri, *Phys. Rev. B* **2001**, *64*, 075206; b) E. Peeters, P. A. van Hal, J. Knol, C. J. Brabec, N. S. Sariciftci, J. C. Hummelen, R. A. J. Janssen, *J. Phys. Chem. B* **2000**, *104*, 10174.

[6] a) P. A. van Hal, R. A. J. Janssen, G. Lanzani, G. Cerullo, M. Zavelani-Rossi, S. De Silvestri, *Chem. Phys. Lett.* **2001**, *345*, 33; b) P. A. van Hal, J. Knol, B. M. W. Langeveld-Voss, S. C. J. Meskers, J. C. Hummelen, R. A. J. Janssen, *J. Phys. Chem. A* **2000**, *104*, 5974.

[7] a) T. Yamashiro, Y. Aso, T. Otsubo, H. Tang, Y. Harima, K. Yamashita, *Chem. Lett.* **1999**, 443; b) S. Knorr, A. Grupp, M. Mehring, G. Grube, F. Effenberger, *J. Chem. Phys.* **1999**, *110*, 3502; c) J.-F. Nierengarten, J.-F. Eckert, J.-F. Nicoud, L. Ouali, V. Krasnikov, G. Hadziioannou, *Chem. Commun.* **1999**, 617; d) S.-G. Liu, L. Shu, J. Rivera, H. Liu, J.-M. Raimundo, J. Roncali, A. Gorgues, L. Echegoyen, *J. Org. Chem.* **1999**, *64*, 4884; e) M. Fujitsuka, O. Ito, T. Yamashiro, Y. Aso, T. Otsubo, *J. Phys. Chem. A* **2000**, *104*, 4876; f) M. Fujitsuka, K. Matsumoto, O. Ito, T. Yamashiro, Y. Aso, T. Otsubo, *Res. Chem. Intermed.* **2001**, *27*, 73; g) L. Segura, N. Martin, *J. Mater. Chem.* **2000**, *10*, 2403; h) J. L. Segura, R. Gómez, N. Martín, C. Luo, D. M. Guldi, *Chem. Commun.* **2000**, 701; i) I. B. Martini, B. Ma, T. Da Ros, R. Helgeson, F. Wudl, B. J. Schwartz, *Chem. Phys. Lett.* **2000**, *327*, 253; j) J.-F. Eckert, J.-F. Nicoud, J.-F. Nierengarten, S.-G. Liu, L. Echegoyen, F. Barigelletti, N. Armaroli, L. Ouali, V. Krasnikov, G. Hadziioannou, *J. Am. Chem. Soc.* **2000**, *122*, 7467; k) S. Komamine, M, Fujitsuka, O. Ito, K. Moriwaki, T. Miata, T. Ohno, *J. Chem. Phys.* **2000**, *104*, 11497; l) N. Armaroli, F. Barigelletti, P. Ceroni, J.-F. Eckert, J.-F. Nicoud, J.-F. Nierengarten, *Chem. Commun.* **2000**, 599; m) M. Yamazaki, Y. Araki, M. Fuijtsuha, O. Ito, *J. Phys. Chem. A.* **2001**, *105*, 8615; n) S.-G. Liu, C. Martineau, J.-M. Raimundo, J. Roncali, L. Echegoyen, *Chem. Commun.* **2001**, 913; o) T. Ono, K. Moriwaki, T. Miyata, *J. Org. Chem.* **2001**, *66*, 3397; p) C. Martineau, P. Blanchard, D. Rondeau, J. Delaunay, J. Roncali, *Adv. Mater.* **2002**, *14*, 283; q) D. M. Guldi, C. Luo, A. Schwartz, R. Gómez, J. L. Segura, N. Martin, C. Brabec, N. S. Sariciftci, *J. Org. Chem.* **2002**, *67*, 1141; r) M. Fujitsuka, A. Masahura, H. Kasai, H. Oikawa, H. Nakanishi, O. Ito, T. Yamashiro, T. Otsubo, *J. Phys. Chem. B* **2001**, *105*, 9930; s) J. Ikemoto, K. Takimiya, T. Otsubo, M. Fujitsuka, O. Ito, *Org. Lett.* **2002**, *4*, 309; t) D. González-Rodriguez, T. Torres, D. M. Guldi, J. Rivera, L. Echegoyen, *Org. Lett.* **2002**, *4*, 335; u) T. Gu, D. Tsamouras, C. Melzer, V. Krasnkov, J.-P. Gisselrecht, M. Gross, G. Hadziioannou, J.-F. Nierengarten, *ChemPhysChem* **2002**, 124; v) D. Hirayama, K. Takimiya, Y. Aso, T. Otsubo, T. Hasobe, H. Yamada, H. Imahori, S. Fukuzumi, Y. Sakata, *J. Am. Chem. Soc.* **2002**, *124*, 532.

[8] For reviews, see a) H. Imahori, Y. Sakata, *Eur. J. Org. Chem.* **1999**, 2445; b) N. Martín, L. Sánchez, B. Illescas, I. Pérez, *Chem. Rev.* **1998**, *98*, 2527; c) H. Imahori, Y. Sakata, *Adv. Mater.* **1997**, *9*, 537; d) M. Prato, *J. Mater. Chem.* **1997**, *7*, 1097.

[9] D. M. Guldi, *Chem. Soc. Rev.* **2002**, *31*, 22, and references therein.

[10] a) R. M. Williams, M. Koeberg, J. M. Lawson, Y. Z. An, Y. Rubin, M. N. Paddon-Row, J. W. Verhoeven, *J. Org. Chem.* **1996**, *61*, 5055; b) K. A. Jolliffe, S. J. Langford, M. G. Ranasinghe, M. J. Shephard, M. N. Paddon-Row, *J. Org. Chem.* **1999**, *64*, 1238; c) K. G. Thomas, V. Biju, D. M. Guldi, P. V. Kamat, M. V. George, *J. Phys. Chem. A* **1999**, *103*, 10755.

[11] a) E. Dietel, A. Hirsch, E. Eichhorn, A. Rieker, S. Hackbarth, B. Röder, *Chem. Commun.* **1998**, 1981; b) D. I. Schuster, P. Cheng, S. R. Wilson, V. Prokhorenko, M. Katterle, A. R. Holzwarth, S. E. Braslavsky, G. Klihm, R. M. Williams, C. Luo, *J. Am. Chem. Soc.* **1999**, *121*, 11599; c) D. M. Guldi, L. Cuo, M. Prato, E. Dietel, A. Hirsch, *Chem. Commun.* **2000**, 373; d) D. M. Guldi, C. Luo, M. Prato, A. Troisi, F. Zebretto, M. Scheloske, E. Dietel, W. Bauer, A. Hirsch, *J. Am. Chem. Soc.* **2001**, *123*, 9166; e) N. Armaroli, G. Marconi, L. Echegoyen, J.-P. Bourgeois, F. Diederich, *Chem. Eur. J.* **2000**, *6*, 1629.

[12] P. Blanchard, B. Jousselme, P. Frère, J. Roncali, *J. Org. Chem.* **2002**, *67*, 3961.

[13] Y. Wei, Y. Yang, J-M. Yeh, *Chem. Mater.* **1996**, *8*, 2659.

[14] C. Bingel, *Chem. Ber.* **1993**, *126*, 1957.

[15] a) A. Hirsch, I. Lamparth, H. R. Karfunkel, *Angew. Chem.* **1994**, *106*, 453; *Angew. Chem. Int. Ed. Engl.* **1994**, *33*, 437; b) A. Hirsch, I. Lamparth, T. Grosser, *J. Am. Chem. Soc.* **1994**, *116*, 9385.

[16] a) D. M. Guldi, M. Prato, *Acc. Chem. Res.* **2000**, *33*, 695; b) D. M. Guldi, K.-D. Asmus, *J. Phys. Chem. A* **1997**, *101*, 1472.

[17] Iodoethane is used as a co-solvent to enhance spin–orbit coupling.

[18] a) Y. Zeng, L. Biczok, H. Linschitz, *J. Phys. Chem.* **1992**, *96*, 5237; b) R. M. Williams, J. M. Zwier, J. W. Verhoeven, *J. Am. Chem. Soc.* **1995**, *117*, 4093.

[19] a) J. Seixas de Melo, L. M. Silva, L. G. Arnaut, R. S. Becker, *J. Chem. Phys.* **1999**, *111*, 5427; b) S. Rentsch, J. P. Yang, W. Paa, E. Brickner, J. Scheidt, R. Weinkauf, *Phys. Chem. Chem. Phys.* **1999**, *1*, 1707.

[20] A. Weller, *Z. Phys. Chem. Neue Folge* **1982**, *133*, 93.

[21] Similar values have been reported for the fullerene reference compounds in ref. [16b] and for a related α-quaterthiophene in ref. [26].

[22] The quenching factor Q_A(D*A) is defined as the ratio of the photoluminescence intensities of the acceptor chromophore (A) after excitation of the isolated acceptor chromphore and after excitation of the donor chromophore (D) of the dyad (DA), after correction for the optical density.

[23] V. Wintgens, P. Valat, F. Garnier, *J. Phys. Chem.* **1994**, *98*, 228.

[24] The absorptions of the $T4^{\bullet+}$ radical cation were determined at 0.98 and 1.74 eV by measuring a 1/1 mixture of **4TP** and TCNE (oxidizing agent which has no absorptions in the infrared region) by PIA spectroscopy.

[25] All reported intensities of the PIA bands ($-\Delta T/T$) were obtained by recording the PIA spectrum at 275 Hz and pumping the sample at 528 nm with 25 mW.

[26] R. S. Becker, J. Seixas de Melo, A. L. Maçanita, F. Elisei, *J. Phys. Chem.* **1996**, *100*, 18683.

[27] a) D. M. Guldi, H. Hungerbuhler, E. Janata, K. D. Asmus, *J. Phys. Chem.* **1993**, *97*, 11258; b) J. W. Arbogast, A. P. Darmanyan, C. S. Foote, Y. Rubin, F. N. Diederich, M. M. Alvarez, S. J. Anz, R. L. Whetten, *J. Phys. Chem.* **1991**, *95*, 11.

[28] The frequency dependence shows the presence of long-lived species by the decay of $-\Delta T$ at low frequencies together with a region at high frequencies where the slope of $-\Delta T$ vs frequency approaches zero, indicating the simultaneous presence of short-lived species. Note that the PIA spectrum itself is measured at 275 Hz, which is already in the latter region.

[29] F. van Bolhuis, H. Wynberg, E. E. Havinga, E. W. Meijer, E. J. G. Staring, *Synth. Met.* **1989**, *30*, 381.

[30] G. Horowitz, B. Bachet, A. Yassar, P. Lang, F. Demanze, J.-L. Fave, F. Garnier, *Chem. Mater.* **1995**, *7*, 1337.

  0947-6539/02/0823-5428 $ 20.00+.50/0

[31] a) R. A. Marcus, *J. Chem. Phys.* **1956**, *24*, 966; b) R. A. Marcus, *J. Chem. Phys.* **1965**, *43*, 679 – 701; c) N. Sutin, R. A. Marcus, *Biochim. Biophys. Acta* **1985**, *811*, 265; d) R. A. Marcus, *Angew. Chem.* **1993**, *105*, 1161; *Angew. Chem. Int. Ed. Engl.* **1993**, *32*, 1111.

[32] This estimate is probably an upper limit to the actual internal reorganization energy in **4TsC** and **4TdC**, as a positive charge will delocalize over a large π-conjugated system to result in in a small structural deformation and reorganization energy.

[33] a) H. Oevering, M. N. Paddon-Row, M. Heppener, A. M. Oliver, E. Cotsaris, J. W. Verhoeven, N. S. Hush, *J. Am. Chem. Soc.* **1987**, *109*, 3258; b) J. Kroon, J. W. Verhoeven, M. N. Paddon-Row, A. M. Oliver, *Angew. Chem.* **1991**, *103*, 1398; *Angew. Chem. Int. Ed. Engl.* **1991**, *30*, 1358.

Received: April 15, 2002 [F4015]

  0947-6539/02/0823-5429 $ 20.00+.50/0